STUDY OF THE KINETICS OF THE ORDER DISORDER TRANSFORMATION IN THE ALLOY $MnNi_3$

Thesis by

Eugene Yu-Cheng Loh

In Partial Fulfillment of the Requirements

For the Degree of

Doctor of Philosophy

California Institute of Technology

Pasadena, California

1954

ACKNOWLEDGEMENT

The author wishes to express his deep appreciation for the advice and constant encouragement given him by Professor Pol Duwez during the course of the present investigation. Furthermore the author expresses his thanks to the staff of the Materials Section of the Jet Propulsion Laboratory for providing him with the samples used in this investigation.

Abstract

$MnNi_3$ is one of many alloys, which, in equilibrium, have disordered (random) and ordered atomic arrangements at temperatures above and below the so-called transition temperature respectively.

Specimens of $MnNi_3$, previously quenched from a temperature at which the structure is disordered, were heated at different constant temperatures below the transition temperature. The magnetization and resistance of these specimens were measured after different intervals of time at these temperatures for the purpose of obtaining data for a study of the kinetics of the isothermal ordering process.

The mechanism of the isothermal ordering process of $MnNi_3$ can be interpreted as first local ordering and then the growth of ordered domains. This mechanism is the same as that qualitatively described by Sykes in 1935 for $AuCu_3$. The mechanism of the local ordering, however, is viewed in the present work as the sharpening of the Gaussian distribution curve of local composition within the alloy.

Previous studies on the kinetics of ordering in $MnNi_3$, AuCu, CoPt and $AuCu_3$ are also reviewed and analyzed; and three different types of ordering mechanisms are proposed.

TABLE OF CONTENTS

LIST OF TABLES

LIST OF FIGURES

I. Introduction

Some alloys can be in different states of order, ranging from the fully ordered state to the completely disordered state. When the alloy is in the fully ordered state, different kinds of atoms are arranged in a definite pattern on the array of atomic sites. When the alloy is in the completely disordered state, these atoms are distributed randomly on lattice points.

The purpose of the present work is to study the kinetics of isothermal ordering of $MnNi_3$, i. e. the manner in which the atomic arrangement of disordered $MnNi_3$ changes to the ordered atomic arrangement. The method of analysis used in this investigation is also applied to the kinetic data of previous investigators to establish the kinetics of ordering in the alloys AuCu, CoPt and $AuCu_3$.

II. Order-Disorder Transformation

A. Ordered and Disordered States

In some binary alloys of composition corresponding approximately to 1 to 1 (AB) or 1 to 3 (AB_3) atomic ratios a change in atomic arrangement takes place at a certain temperature, which is called the transition temperature. Below this temperature the structure is ordered and above it is disordered. In an ordered alloy the different kinds of atoms are arranged in a definite pattern on the array of atomic sites and usually atoms of one species tend to surround themselves by atoms of the other species. Consequently the internal energy and also the free energy of the alloy at low temperature are decreased by the ordering process. In the disordered alloy atoms of different kinds are distributed randomly on lattice points, with the result that the entropy of the alloy is large. Hence the free energy at high temperatures is lower for the disordered alloy than for the ordered alloy. Since minimum free energy is the requirement for equilibrium, at each temperature the alloy has a definite state of order. This fact is confirmed both theoretically and experimentally.

One conclusive evidence of an ordered arrangement is furnished by the presence of "superlattice lines" on x-ray diffraction patterns. Superlattice lines are

reflections from the new and larger spacings, which are present in patterns of ordered alloys only. These new and larger spacings are caused by the distribution between different sets of lattice points. In the ordered alloy, each set contains all the atoms of one species and atoms in different sets are different from each other. In the disordered alloy the distribution of atoms on lattice points is statistically random and hence there is no distinction between lattice points.

Surprisingly enough the first suggestion of the existence of ordered structures was based not on x-ray evidence but on the chemical behavior of AuCu solid solutions. In 1919, Tammann (1) found that in gold-copper alloys containing more than 50 atomic per cent Cu the copper in excess of 50 per cent was rapidly dissolved by nitric acid. He concluded that the alloy having the stoichiometric composition AuCu contained an ordered arrangement of atoms and the extra Cu-atoms which did not fit into this arrangement were easily removed.

The first direct observation of superlattice lines in x-ray diffraction pattern of $AuCu_3$ was reported by Bain in 1923 (2). The first analysis of an ordered structure from its x-ray pattern was made by Johansson and Linde for the alloy AuCu in 1925 (3).

Following these investigations, order-disorder reactions have been found in many alloy systems.

Comprehensive review papers on this subject were written by Nix and Shockley in 1938 (4) and by Lipson in 1950 (5).

B. Crystal Structure and Properties of Ordered and Disordered Alloys

The difference in the atomic arrangements in ordered and disordered alloys leads to different crystal structures. The fundamental important types of lattice change from the disordered to the ordered structures, which are shown in Fig. 1, for substitutional binary alloys are as follows (5):

AB type

i. Body-centered cubic to simple cubic of same size unit cell such as β brass and FeAl.

ii. Face-centered cubic to tetragonal with like atoms on alternate planes, examples being AuCu and CoPt.

AB_3 type

i. Face-centered cubic to simple cubic of same size unit cell. In the ordered structure the A-atoms are on one set of lattice points and the B-atoms are on the other three sets*, examples being $AuCu_3$ and $MnNi_3$.

ii. Body-centered cubic to face-centered cubic of twice the original lattice parameter with A-atoms arranged at corners of the tetrahedron,

---

* The face-centered cubic structure can be considered as four interpenetrating simple cubic structures.

these corners are located at body-centers of the disordered cubic system. Fe_3Al is an example.

iii. Hexagonal close packed to hexagonal having an a parameter twice that of the disordered hexagonal cell, but the same c parameter, examples being Mg_3Cd and $MgCd_3$.

The physical properties of an alloy also change as a consequence of ordering. Examples of properties influenced by the atomic rearrangements are: Anomalous specific heat near the transition temperature, heat of evolution on ordering arising from the fact that the ordered alloy has less internal energy than that of the disordered one, elastic modulus, hardness, density, color, electrical resistivity, thermoelectric power, susceptibility and other magnetic properties. In some cases, the ordering introduces lattice strains, which can be observed under the microscope as striations on a polished surface. For a particular alloy, only a few of the above-mentioned properties change appreciably during the ordering process, and those properties which do vary considerably on ordering are generally used for measuring the state of order of the alloy.

C. The Kinetics of Ordering

The mechanism by which the change from a disordered to an ordered structure occurs depends on the type of alloy, its past history, and the time and temperature of ordering. In some alloys the change from the disordered to the ordered state is almost instantaneous, in others the reaction may be extremely slow.

Since some of the physical properties of an alloy and its x-ray diffraction pattern are influenced by the atomic arrangement, they can be used as an indirect measure of the state of order.

The first problem in the study of ordering kinetics is to establish a relation between the state of order and the measured physical properties. These measurements are usually taken at room temperature from the quenched specimen, since the atomic arrangement existing at the ordering temperature can be retained in most alloys by quenching. The diffusion rate at room temperature is negligible. The second problem is to find a relation between the variation of the measured physical properties with time, temperature and other relevant factors.

III. Survey of Previous Work on the Kinetics of Ordering

Most of the previous studies of ordering kinetics, as shown in Table I, have been concerned with change in physical properties with time during isothermal ordering. In several of these studies, the total length of time at a given temperature was too short to reach a state of equilibrium. Alloys studied were of the AB and AB_3 types with the disordered structure being face-centered cubic, the ordered structure being tetragonal and simple cubic respectively.

Table I

Alloy	Physical Properties Measured	Investigators
AuCu	Heat of evolution	Borelius and
	Intensity and displacement of	collaborators
	x-ray diffraction line	(6, 7, 8)
	Electrical resistance	Diennes (9)
	Axial ratio of ordered AuCu	Gorsky (10)
	X-ray and microstructure	Harker (11)
CoPt	Electrical resistance	Newkirk et al
	Hardness	(12)
	Magnetic properties	
	X-ray and microstructure	
CuPt	Hardness	Nowack (13)
$AuCu_3$	Electrical resistance	Sykes et al
	Width of superlattice line	(14, 15, 16)
	Elastic modulus	Siegel (17)
$MnNi_3$	Electrical resistance	Thompson (18)
	Magnetization	

Borelius and his collaborators investigated the kinetics of ordering of AuCu by studying the x-ray diffraction patterns (8). From their results the ordering process of AuCu, from disordered face-centered cubic to ordered tetragonal structure, seems to occur in two different ways. First, near the transition temperature the disordered structure may gradually disappear, being replaced by the ordered structure; this effect would be evidenced by a gradual decrease of the intensity of the (311) cubic reflection, and a gradual increase of the intensity of the (311) tetragonal reflection, no change being observed in the Bragg angle (8). Second, at temperatures considerably lower than the transition temperature the axial ratio c/a may change gradually from unity to the equilibrium value; and this effect would be evidenced by a gradual shift of the (311) cubic reflection to its position for the equilibrium tetragonal structure (8, 10). Near the transition temperature, 408 C, kinetic data have been obtained for AuCu by measuring the heat of evolution (6, 7) together with the intensity of (311) cubic and tetragonal reflections (8). At low temperatures, between 200 and 300 C, measurements have been made from the displacement of the (311) reflection (8).

Borelius and his collaborators (6, 7, 8) normalized the measurements of physical properties by making the

total change for complete ordering equal to unity. The normalized values were plotted against the log time of ordering at constant temperatures. The activation energy of the process at temperatures away from the transition temperature was obtained by measuring the slope of the straight-line portion of the plot of log time for half of the total change versus the reciprocal of ordering temperature in degrees Kelvin. The retardation of the ordering and disordering process near the transition temperature was explained by the potential barrier for the formation of ordered nuclei. This barrier does not exist at temperatures away from the transition temperature because of the variation in free energy with degree of order (8). Borelius and his collaborators also analyzed the beginning part of their data of heat of evolution and stated that the ordering process of AuCu starts with constant nucleation and constant radial growth of spherical nuclei.

Diennes (9) measured the resistance of AuCu at room temperature during the isothermal ordering process. The specimens used were not completely disordered prior to this treatment. The range of temperature was 250 to 360 C, which is considerably below the transition temperature. The correlation between the resistance and long-range order parameter used by Diennes may not be valid for his

investigation, since the state of order of the specimen during the ordering process can hardly be described by a long-range order parameter alone. The ordering time was not long enough to attain equilibrium, this would have been apparent if the time scale used had been logarithmic instead of linear.

From the wire specimen of $AuCu_3$ Jones and Sykes (15) measured the breadth of superlattice lines during isothermal ordering at 298, 346 and 376 C to determine the size of ordered domain. Also they measured the electrical resistance at room temperature. Their results may be summarized as follows: first, from the plot of size of ordered domain vs. log ordering time, rate of growth are slower in cold-worked specimens than in annealed specimens; second, in the plot of electrical resistance vs. reciprocal of the size of the ordered domain, curves for both annealed and cold-worked specimens become a single straight line for sufficient large domain sizes, say 100 Å at 298 C; third, the boundaries between ordered domains are narrow and are about two interatomic distances wide, 7.5 Å for $AuCu_3$.

Based on the experimental results on $AuCu_3$, the mechanism of isothermal ordering of $AuCu_3$ was qualitatively described by Sykes and Jones as first the local ordering and then the growth of "anti-phase" ordered domains, i. e. domains which are not in registry.

A previous study of ordering kinetics of $MnNi_3$ appears primarily in Thompson's paper (18). He obtained some kinetic data for $MnNi_3$ by measuring resistance and magnetization of the specimen both at room temperature and at the ordering temperature. Thompson qualitatively described the mechanism of ordering of $MnNi_3$ following the concept that Sykes proposed for $AuCu_3$ (15), first local ordering and then the growth of "anti-phase" ordered domains. The time scale used in the plot of measured physical porperties was linear, and probably equilibrium was not reached.

It can be seen from this survey that most of the previous data have not been analyzed to describe the kinetics of isothermal ordering. Only the beginning part of the ordering process of AuCu near the transition temperature has been analyzed by Borelius and his collaborators (6, 7). In section VII of this thesis isothermal ordering data will be analyzed and the ordering process will be described, as is done in section VI for the present investigation on $MnNi_3$.

IV. Experimental Technique

The temperature of order-disorder transformation in the alloy corresponding to composition $MnNi_3$ is 510 C as shown in Fig. 2. The disordered crystal structure is face-centered cubic with each lattice point occupied randomly by either manganese or nickel atoms. The ordered structure is simple cubic with Mn-atoms on one set of lattice points and Ni-atoms on the other three sets, as discussed on page 4 and shown in Fig. 1.

A. Preparation of Specimens

Specimens used in the experiments were prepared by the Materials Section of the Jet Propulsion Laboratory of California Institute of Technology.

Nickel and manganese powders were mixed and pressed to a bar 3/8 in. square and 1 in. long under a pressure of 80,000 pounds per square inch. The bar was sintered 4 hours at 980 C, in hydrogen, quenched in water and then reduced in cross section by about 20 per cent by cold rolling. This procedure was repeated twice. The densely packed $\frac{1}{4}$ in. square bars were turned to disks of 1/8 in. dia. x 1/16 in. thickness or rolled to strips of 0.008 in. x 1/8 in. x $1\frac{1}{2}$ in. The disks were used for magnetization measurements and the strips for resistance measurements. The specimens were sealed in evacuated quartz tubes. They were then heated about 10 minutes at 980 C and quenched in water to retain the disordered Structure.

B. Isothermal Ordering of the Specimen

The isothermal ordering of the specimens was accomplished by heating the vacuum-sealed specimens in copper blocks in automatically controlled furnaces at constant temperatures. The average temperature fluctuation of these furnaces was about ±3 C during these thermal treatments. Some magnetization data were obtained from specimens not sealed under vacuum, since there was no detectable difference in magnetization data between the vacuum-sealed and non-sealed specimens.

C. Measurement of Magnetization

The magnetization of isothermally ordered specimens was measured at room temperature with a magnetic torsion balance shown in Fig. 3. Readings on dials, 1 and 2, correspond to the twist of the vertically suspended steel wire, 3, whose upper end is fastened on the dial, 1, and whose lower end is fixed to the frame. The torsional moment produced by the elastic twist of this steel wire, 3, balances that of the magnetic force acting on the specimen. The specimen is fastened at the end, 5, of the aluminium rod, 4, and is located in the middle of the convergent magnetic field of the magnetron magnet, 6, which has a field strength of about 2,000 Gauss. The sensitivity of readings on dial, 2, is one hundredth of one degree of the twist of the steel wire, 3, and the accuracy is about one fiftieth of one degree.

Readings on dials, 1 and 2, give the value of magnetization M, which is proportional to the magnetization of the specimen. Since only relative values of change in physical properties are of interest in the study of kinetics of ordering, no unit has been given to the value of M.

D. Measurement of Resistance

The resistance of the isothermally ordered strip specimen was determined at room temperature by comparing the potential E_x across the specimen with the potential E_s across a standard resistor of 0.1 ohm in the same circuit. The resistance of the $MnNi_3$ specimen is thus equal to $0.1(E_x/E_s)$. Fig. 4 shows the wiring diagram used for the measurement of resistance. The standard resistor and the $MnNi_3$ strip specimen are connected in series in a direct current circuit, which is supplied by a 1.5 volt dry cell battery. The current reverse switch permits the reversal of the battery voltage in the circuit, so that the thermocouple effect produced by the temperature differences at different junctions in the circuit are compensated by taking readings with the current reverse switch in both positions. A type K potentiometer is connected by the selector switch to the $MnNi_3$ specimen or to the standard resistor for measuring the potentials E_x and E_s respectively. The sensitivity of this potentiometer is

one microvolt and the readings are reproducible within 0.5 millivolt because of the thermocouple effect in the circuit of the potentiometer. This effect causes only negligible error in the resistance measurements. The more important source of scatter of the resistance data results from the fact that the specimen could not be clamped in exactly the same position in each measurement.

As in the case of magnetization measurements only relative values of resistance are of interest in the study of kinetics.

V. Experimental Results

Magnetization and resistance readings versus logarithm of ordering time at several constant sub-transition temperatures are shown in Fig. 5 and 6 respectively; the data are listed in Table II and III respectively.

Table II

Magnetization Data

Temp. (C)	400 ⊙		416 ▲		443 ⊡	
Spec. No.	156		157		161	
t (min.)	M		t (min.)	M	t (min.)	M
0	0.5		0	0.55	0	0.55
11	1.8		12	2.1	7	1.9
53	2.65		49	2.7	47	3.43
172	4.25		184	4.2	216	7.4
292	5.5		474	6.2	652	12.7
584	7.8		1114	9.4	1394	16.7
1042	10.4		2234	13.1	5916	22.2
2152	14.05		4062	16.15	8711	23.1
3989	17.1		7334	19.3	14957	24.45
7261	19.9		15589	21.6	22159	25.14
10635	21.2		26567	23.16	34525	25.75
14730	21.77		50679	25.25	70365	26.61
24283	23.17		82459	25.81	93352	26.9
47198	24.4		124279	26.18		
78963	25.4					
125263	26.09					
M_i	1.5		1.9		1.9	
M_1	23		22		22	
M_2	28		29		28.5	

Table II (continued)

Magnetization Data

Temp. (C)	460 ✱		488 ▼		506 ⊕	
Spec. No.	170		154		152	
t (min.)	M	t (min.)	M	t (min.)	M
0	0.5	0	0.4	0	0.45
10	1.89	6	1.85	16	3.55
34	3.41	15	2.7	43	5.9
92	5.88	54	5.9	119	9.15
150	7.75	402	14.45	330	11.8
278	10.73	1005	17.2	1168	13.95
506	13.87	1965	18	3631	15.3
766	15.64	4678	19.7	7599	16.05
1366	17.7	8209	20.65	10120	16.25
2874	20.08	11478	20.8	15374	16.25
5723	21.2	19313	21.3		
8799	22.36	22908	21.6		
13096	23.1	38143	21.83		
20061	23.6	69933	22.25		
		86833	22.46		
M_i	1.7		1.7		2
M_1	20		18		13
M_2	25.5		23		17.5

Table II (continued)

Magnetization Data

Temp. (C)	503 x
Spec. No.	A15
t (min.)	H
0	0.72
6	1.31
17	1.88
29	2.24
51	2.81
98	3.86
166	4.32
293	5.62
524	6.4
774	6.98
1325	7.28
2183	7.65
3184	7.94
4868	8.13
7304	8.36
13012	8.54
H_i	0.72
H_1	7
H_2	9

Table III

Resistance Data

Temp. (C)	400 ⊙		416 ▲	
Spec. No.	R4		R2	
	t (min.)	R (ohm)	t (min.)	R (ohm)
	0	0.031394	0	0.0287008
	2	0.032708	10	0.030410
	7	0.032980	37	0.030635
	17	0.033130	64	0.030645
	51	0.033397	112	0.030411
	121	0.033323	150	0.030663
	708	0.033084	209	0.03045
	1518	0.032770	404	0.030067
	3204	0.032357	775	0.029265
	7277	0.030908	1498	0.027597
	15533	0.026934	3483	0.02447
	42585	0.023671	7434	0.021636
	101815	0.01882	15681	0.019217
	134997	0.01758	34209	0.017204
			60104	0.015839
			101529	0.0154
R_m	0.0334		0.0307	
R_1	0.022		0.022	
R_2			0.013	

Table III (continued)

Resistance Data

Temp. (C)	452 +		488 ▼	
Spec. No.	R10		R3	
	t (min.)	R (ohm)	t (min.)	R (ohm)
	0	0.0337	0	0.028624
	4	0.03577	10	0.030327
	9	0.03585	38	0.030071
	19	0.036	66	0.029638
	40	0.03585	108	0.029373
	70	0.03517	178	0.028618
	127	0.0349	370	0.027534
	212	0.0345	735	0.027003
	373	0.0334	1457	0.025988
	537	0.0319	4030	0.025720
	772	0.0304	7972	0.025553
	1046	0.0295	16214	0.025255
	1598	0.0282	34209	0.025235
	2580	0.027	60104	0.025
	4125	0.02607	78564	0.02444
	8070	0.025		
	16283	0.024		
	28708	0.0235		
	46383	0.0231		
R_m		0.036		0.0303
R_1		0.032		0.027
R_2		0.022		0.025

VI. Discussion of Kinetic Data

A. Magnetization Measurements

i. Specimens quenched from above the transition temperature.

Magnetization data obtained by heating specimens for various lengths of time at constant temperature are plotted in Fig. 5. Each of these curves can be approximated by two straight lines corresponding to two steps during the ordering process as shown in Fig. 7. The first step, local ordering, is plotted as $\ln\ln(1-f_1)^{-1}$ vs. $\ln(t)$ and is fitted by solid straight lines; and the second step, corresponding to the growth of anti-phase ordered domains, is plotted as $\ln(1-f_2)$ vs. $\ln(t)$ and is fitted by dashed straight lines. The parameter f_1, equal to $(M-M_i)/(M_1-M_i)$, is a dimensionless parameter representing the fractional change in magnetization readings during the local ordering. The value of f_1 is zero near the beginning of the ordering process, where $M=M_i$, and is unity near the end of the local ordering, where $M=M_1$. Similarly f_2, equal to $(M-M_i)/(M_2-M_i)$, is a dimensionless parameter representing the fractional change of magnetization reading during the second stage of the ordering process. As in the case of f_1 the value of f_2 is zero near the beginning of the ordering process, where $M=M_i$, and is unity, with the magnetization reading $M=M_2$, when

the specimen reaches the state of equilibrium at the ordering temperature. Values of M_i and M_2 can be directly estimated from the beginning and the end, respectively, of the isothermal curve in Fig. 5. The value M_1, however, is obtained by plotting the magnetization data as $\ln(1-f_2)$ vs. $\ln(t)$. At greater values of ordering times, the magnetization data are fitted by a straight line with slope -0.5. A plot of this kind is illustrated in Fig. 8 for a specimen heated at 443 C. As is seen in this figure, the straight line AB can be used to fit the data after 5,700 minutes. But the part of the data corresponding to times less than 5,700 minutes does not fall on this straight line and $\ln(1-f_2)$ approaches the value $\ln(1)$ asymptotically as time is decreased to zero. This deviation of the early part of the data from the straight line means that the plot of $\ln(1-f_2)$ vs. $\ln(t)$ is not suitable for describing the local ordering. The point A in Fig. 8, where the plotted data start to deviate from a straight line, is taken as representing the end of the first part of the ordering process; consequently, the magnetization reading corresponding to this point is taken as equal to M_1. It is realized that the determination of the value of M_1 is not precise. However, a consistent method for locating the deviation points in plots similar to that shown in Fig. 8 was used for all magnetization curves.

After a value was chosen for M_1, the data corresponding to the first part of the ordering process were plotted as shown in the left part of Fig. 7. This part of the data is plotted as $\ln\ln(1-f_1)^{-1}$ vs. $\ln(t)$, and these data fall on a straight line with slope equal to 0.75 (cf. solid lines in Fig. 7). The linearity of the plot in this part of the ordering process leads to an expression of the type:

$$\ln \ln 1/(1-f_1) = \ln (\text{const.} \quad t^{0.75}) \qquad (1)$$

The differential form of equation (1) is:

$$\Delta f_1 = \text{const.} \ (1-f_1)\Delta(t^{0.75}) \qquad (2)$$

The following discussion may explain the first step of the ordering mechanism of $MnNi_3$ corresponding to equation (2).

Atoms in the alloy $MnNi_3$ may be considered to form groups, within which the concentration w of alternate regions of equal size fluctuates because of thermal agitation. In one region the concentration becomes $w+\Delta w$ and in the immediately adjacent region the concentration becomes $w-\Delta w$. At equilibrium the number of atoms, n, in these two regions presumbly depends on the temperature of the specimen and is a result of a balance between the ordering effect due to the interatomic actions and the disordering effect due to the thermal agitation. At high

temperature the number of atoms involved in a fluctuating group is small because of strong thermal agitation. Conversely the number of atoms in a fluctuating group is large at low temperature.

The state of order of the alloy may be approximately described by the Gaussian distribution of the composition in fluctuating groups. The probability P of a fluctuating group having composition between $(w \pm \Delta w)$ and $(w \pm \Delta w) + dw$ is given as (20):

$$P = \sqrt{\frac{n}{\pi}\left(\frac{zV}{kT} + \frac{1}{2w(1-w)}\right)}\; e^{-\frac{1}{2}\frac{n}{kT}\frac{d^2f}{dw^2}(\Delta w)^2} dw \qquad (3)$$

The peak of the Gaussian distribution, where the local composition is equal to the average composition w of the alloy, is given by:

$$\sqrt{\frac{n}{\pi}\left(\frac{zV}{kT} + \frac{1}{2w(1-w)}\right)}$$

or for $MnNi_3$

$$\sqrt{\frac{n}{\pi}\left(\frac{zV}{kT} + \frac{8}{3}\right)} \qquad (4)$$

If the local composition is 25 atomic per cent of Mn, then the local degree of order is high. Hence expression (4) corresponds to the portions of the alloy which are fully ordered. When the temperature is high and consequently the number of atoms n in the fluctuating group is small, expression (4) has a small numerical value and therefore the Gaussian curve is flat.

The first step of the isothermal ordering process corresponds to changing a flat Gaussian distribution curve (characteristic of a disordered state) into a sharp one (characteristic of an ordered state) by increasing the number of atoms in the fluctuating group. This increase is the result of stronger interactions between atoms at the ordering temperature. The probability of composition fluctuations is reduced for larger fluctuating groups and thus the degree of local order is increased.

The magnetization reading may be assumed to be proportional to the area of a narrow strip under the peak of the Gaussian distribution curve. A reason for this assumption may be found in a paper by Smoluchowski (21), who computed the saturation magnetization of ordered and disordered alloys from their local electron concentration by using the Pauling-Shockley curve of saturation magnetization versus electron concentration. The computed results agreed generally well with the experimental data. The contributions of the Ni-Ni pair, Ni-Mn pair, and Mn-Mn pair interactions to the saturation magnetization of the disordered $MnNi_3$ alloy were determined to be 0.71, 0, and some unknown negative number of Bohrmagnetons respectively. In order to explain why the disordered $MnNi_3$ alloy has a very small saturation magnetization whereas the ordered alloy has a very large one, one may suggest that the magnetization of $MnNi_3$ would be propor-

tional to the portion of the alloy in which the concentration of Mn is very close to 25 atomic per cent. The contribution of the regions in which the concentration of Mn is either smaller or larger than 25 per cent cancel each other. The magnetization reading is thus proportional to the area of a narrow strip underneath the peak of the Gaussian distribution curve of composition. Expression (4) shows that this area is proportional to $n^{\frac{1}{2}}$ during the isothermal ordering process, since all parameters in (4) except n are constant. If the number of atoms, n, in the fluctuating group increases as $t^{1.5}$ in the disordered matrix, as in the case of the growth of spherical particles by diffusion (22), then the increment of the magnetization reading is proportional to the product of the mass of the available disordered region and the increment of $n^{\frac{1}{2}}$. Equation (2) may be explained, since the available disordered region is proportional to $(1-f_1)$ and the increment of $n^{\frac{1}{2}}$ is proportional to the increment of $(t^{1.5})^{\frac{1}{2}}$.

A physical interpretation of the second step of the ordering process will now be attempted. As shown in Fig. 7 the data describing the change of magnetization during this step in the ordering process lie on a straight line with slope -0.5 (dashed lines in the right-hand part of Fig. 7). The coordinates of the plot are $\ln(1-f_2)$ and $\ln(t)$, where

$$f_2 = (M-M_i)/(M_2-M_i)$$

is the fraction of change in magnetization during the ordering process. The equation of this linear portion of the plot is:

$$\ln (1-f_2) = \ln (\text{const. } t^{-0.5}) \qquad (5)$$

Its differential form is:

$$\Delta f_2 = - \text{const. } \Delta(t^{-0.5}) \qquad (6)$$

During this period of the ordering process the increase in the magnetization is presumbly the result of the decrease in the mass of the disordered domain-boundaries. These boundaries are progressively absorbed by the growth of anti-phase ordered domains, which are not in registry with one another. According to the results of Sykes (15) as mentioned in section III the domain-boundary has a constant thickness during the course of the growth of the ordered domains. The mass of domain-boundaries with constant thickness is inversely proportional to the size of the domain, the size of the domain being defined as some linear dimension of the domain. This proportionality is true at least for domains having cubic shape and should be also true, to the first approximation, for domains with other ordinary shapes. If the growth of the size of an ordered domain is assumed to be proportional

to $t^{\frac{1}{2}}$ (as discussed in section VII for $AuCu_3$), then the increase in magnetization reading in this step of the process is given by equation (6).

The change in magnetization during the second stage of the ordering process is about one third of the total change. Since the change in magnetization in this stage of the process is caused by the growth of the ordered domains, the domain size at the beginning of this stage of the process can be estimated as follows. Assume, for simplicity, that the domain is cubic in shape, and initially has d atoms along each edge of the cube. Also, let the thickness of the domain-boundaries e be equal to two atomic distances during the growth of the domains as verified by Sykes (15). Then the fraction of magnetization increase during this stage of the process, which amounts to 1/3, is equal to the fractional increase of the ordered volume of the domain, namely:

$$1/3 = 1 - 6ed^2/d^3$$

since the cubic domain has six faces of disordered boundary. The domain-size at the beginning of the second stage of the process is thus estimated as 18 atomic distances from the above equation, which was used by Sykes for $AuCu_3$.

From the above analysis of the kinetic data of magnetization, the isothermal ordering process of $MnNi_3$ may be considered to consist of first the local ordering, being described in the present work as the sharpening of the Gaussian distribution curve, and then the growth of the anti-phase ordered domains. These two steps of ordering process were first qualitatively suggested by Sykes and his collaborators in 1935 (14, 15, 16) for $AuCu_3$. Since the crystal structures of both ordered and disordered $AuCu_3$ and $MnNi_3$ are same, the ordering mechanism of these two alloys might be the same.

ii. Influence of initial magnetization reading.

Specimens quenched from the same high temperature should have the same low initial magnetization reading. However, because of slight discrepancies in compositions from specimen to specimen or because of small variations in quenching rates, the initial magnetization readings of quenched specimens may not be exactly the same. For example, the initial magnetization of specimens quenched from 980 C ranges from 0.35 to 0.60; when specimens were quenched from 543 C, the range was from 0.55 to 1.33, the order-disorder transition temperature being at 510 C. For the purpose of investigating the influence of the initial magnetization reading on the ordering kinetics, specimens quenched from the same temperature (but having slightly different initial magnetizations) were heated simultaneously for various lengths of time at the same ordering temperature. Four pairs of isothermal curves are shown in Fig. 9. Each pair of these curves shows that the magnetization curve of the specimen having the lower initial magnetization (full line curve) rises faster and eventually is higher than that of the specimen having the higher initial magnetization during the first part of the ordering process (local ordering). During the second part of the process (growth of the anti-phase domains), however, magnetization readings of both specimens rise in the same manner.

These observations may be explained by assuming that the higher the initial magnetization reading, the larger is the number of ordered nuclei in the specimen. The growth of ordered nuclei is negligible during the first part of the process, which corresponds to the local ordering. These nuclei however are surrounded by disordered boundaries, and presumbly these boundaries counteract the ordering process. Therefore, the first part of the ordering process is retarded in a specimen having initially a large number of such nuclei.

iii. Specimens having been partially ordered.

The experiments described previously were made with specimens in which the initial degree of order was as small as possible, since these specimens were quenched from high temperature. It can be shown that the specimens having a certain degree of order before the isothermal ordering treatment can be described by the same analytical treatment as for specimens quenched from above the transition temperature.

Some specimens were partially ordered at a temperature of 493 C, the transition temperature being at 510 C. Following this treatment, the kinetics of isothermal ordering at some lower temperature, as 443 C, was studied. As was done in Fig. 7 for the data obtained from specimens quenched from above the transition temperature, during the first step of the ordering process the data are plotted as $\ln\ln 1/(1-f_1)$ vs. $\ln(t)$, to which is fitted a straight line of slope 0.75; and during the second step of the ordering process the data are plotted as $\ln(1-f_2)$ vs. $\ln(t)$ and can be fitted by a straight line with slope -0.5. Thus the ordering process for specimens previously partially ordered is presumbly the same as that of the specimens quenched from above the transition temperature. The isothermal ordering process of $MnNi_3$ hence always consists of two steps, whether specimens were quenched

from temperatures above or from temperatures below the transition temperature. The first part of the process (local ordering) is the process of changing the local state of order from one corresponding to a higher temperature, either above or below the transition temperature, to that corresponding to the ordering temperature. After the state of order in each domain attains the value corresponding to that for the ordering temperature, the second part of the ordering process is operative, consisting of the growth of anti-phase ordered domains.

iv. Interpretation of results based on the concept of nucleation and growth

One may use the terminology of "nucleation and growth" to describe the first part of the isothermal ordering process of $MnNi_3$. The fact, as shown in Fig. 9, that specimens having initially lower magnetization readings always have higher magnetization readings after a certain ordering time indicates that the "growth" of the ordered region can not be important during this part of the process. In other words, this part of the process can be described as the "nucleation" of ordered domains with negligible "growth" of these ordered domains.

The increase in magnetization reading in this first part of the ordering process can be assumed to be proportional to the number of ordered nuclei. These nuclei have the same size, which is the domain size (18 atomic distances) at the beginning of the second part of the ordering process (growth of ordered domain). Equation (2) can thus be stated in the differential form:

$$\Delta\left(\begin{matrix}\text{Number of}\\ \text{ordered nuclei}\end{matrix}\right) \sim \left(\begin{matrix}\text{Volume available}\\ \text{for nucleation}\end{matrix}\right) \Delta\,(t^{0.75}) \sim (1-f_1)\,\Delta(t^{0.75})$$

The nucleation rate N_e, which is the number of nuclei formed per unit time, is thus:

$$N_e \sim (1-f_1)\,\frac{d\,t^{0.75}}{dt} \sim (1-f_1)\cdot(t^{-0.25}) \qquad (7)$$

Equation (7) may be used to describe the mechanism of isothermal ordering during the first part of the process. The local ordering of $MnNi_3$ is a process of nucleation of ordered domains and the nucleation rate per unit disordered mass, $N_e/(1-f_1)$, is proportional to the $-\frac{1}{4}$ power of the ordering time.

The previous description of the first part of the ordering process, namely the sharpening of the Gaussian distribution curve, affords an explanation of relation (7) and gives a physical interpretation for the time exponent.

B. Electrical Resistance Measurements

Specimens used in the electrical resistance measurements were all quenched from above the transition temperature.

The variation of the electrical resistance with time is shown in Fig. 6. The resistance increases at the beginning of the ordering process then decreases. This initial increase in resistance during the ordering process was also observed by Thompson (18). One might suggest that this anomalous effect is due to the disappearance of internal stress set up during quenching. The present discussion of resistance data does not cover this rising portion of resistance data, which lasts a short portion of the ordering process.

The analysis of data previously used for the magnetization measurements is applied to the electrical resistance measurement data. The curves of Fig. 6 are replotted as shown in Fig. 10. The two sets of straight lines in Fig. 10 correspond to the two steps during the ordering process. These two plots are "$\ln\ln(1-r_1)^{-1}$ vs. $\ln(t)$" and "$\ln(1-r_2)$ vs. $\ln(t)$" for the part of "local ordering" and "growth of anti-phase domains" respectively. The dimensionless parameter r_1, equal to $(R-R_m)/(R_1-R_m)$, represents the fractional change in resistivity during the local ordering; r_1 has the value

zero, when $R=R_m$, near the maximum resistance, and the value one, when $R=R_1$, near the end of the first part of the ordering process. Similarly the parameter r_2, equal to $(R-R_m)/(R_2-R_m)$, is the dimensionless parameter representing the fractional change of resistivity during the second part of the ordering process; it has the value one, when $R=R_2$, at the time the specimen reaches the state of equilibrium at the ordering temperature. Values of R_m and R_2 can be estimated directly from the peak and the end of the isothermal resistance curves in Fig. 6 respectively. The value of R_1 can be obtained by the same procedure used to determine M_1 in Fig. 7. The procedure consists of taking the value of resistance corresponding to the point where the plot deviates from the straight line which fits the later part of the resistance data in the plot of $\ln(1-r_2)$ vs. $\ln(t)$.

As shown in Fig. 10, which is analogous to Fig. 7 for magnetization data, the straight line which fits the data for the first part of the process has a slope equal to 1.25, and the straight line which fits the data for the second part has a slope equal to -0.5. The equations of these two straight lines are:

$$\ln \ln 1/(1-r_1) = \ln (\text{const.}\ t^{1.25}) \qquad (8)$$

$$\ln (1-r_2) = \ln (\text{const.}\ t^{-0.5}) \qquad (9)$$

The time dependence of change in resistivity may then be obtained by differentiating equation (8) and (9) and the following relations are obtained;

$$\Delta r_1 = \text{const.}\ (1-r_1)\ \Delta(t^{1.25}) \qquad (10)$$

$$\Delta r_2 = -\text{const.}\ \Delta(t^{-0.5}) \qquad (11)$$

A probable explanation for the first part of the ordering process, that corresponding to equation (10), is as follows. The change in resistance is proportional to the change in the product of the probability that the conducting electrons hit the ordered region in their path and the cross section of the ordered fluctuating groups. The probability that conducting electrons hit the ordered fluctuating groups is proportional to $t^{0.25}$. This can be shown as follows: This probability is proportional to the linear fraction of ordered fluctuating groups, which in turn is proportional to the 1/3 power of the spatial fraction of ordered fluctuating groups, namely $(n^{\frac{1}{2}})^{\frac{1}{3}}$ or $n^{\frac{1}{6}}$. Since n is proportional to $t^{1.5}$, it may be concluded that the probability that conducting electrons hit the ordered fluctuating groups is proportional to $t^{\frac{1.5}{6}}$, or $t^{0.25}$.

It can be shown that the cross section of the fluctuating group is proportional to the ordering time t. Since the cross section is proportional to the 2/3 power of the volume of the fluctuating group and the volume of the fluctuating group is proportional to the 3/2 power of the time, the cross section of the fluctuating group is therefore proportional to $(t^{\frac{3}{2}})^{\frac{2}{3}}$, namely proportional to t. By combining the time dependence of the above-mentioned probability and the cross section, the change of resistivity in this part of the ordering process is therefore proportional to the change in the product of time t and time to the power 0.25, i. e. proportional to the change of $t^{1.25}$.

The second step of the isothermal ordering process is represented by equation (11) based on the resistance data. The explanation for equation (11) is principally the same as that for equation (6), since both equations (6) and (11) describe the same step of the ordering process and they have the same time dependence. As before, if the number of disordered domain-boundaries is inversely proportional to the size of the ordered domain and if the growth of the ordered domain is proportional to $t^{\frac{1}{2}}$, then equation (11) will be proved by assuming that the decrease in resistance is proportional to the decrease of the number of disordered domain-boundaries per unit length as also mentioned by Sykes (15).

VII. Analysis of Previous Work on Ordering Kinetics

It has been shown in section III, that a number of order-disorder reactions were studied by previous investigators. Various methods of measuring the rate of ordering were used in these studies. Some of the most important kinetic data will now be analyzed to obtain the time dependence of the changes in the particular physical property measured. Then the ordering process will be described by utilizing this time dependence and an assumed relation between the change in physical property and the increase in the ordered mass of the alloy. These procedures of analysis and of interpretation of ordering data are analogous to those used for $MnNi_3$ in the previous section.

A. $MnNi_3$

Thompson's results of magnetization and resistance measurements (Fig. 8 in his paper of reference 18) have been replotted in Fig. 11 using a logarithmic time scale. Evidently the measurements were not carried out for a sufficient length of time and an equilibrium state was not reached. In general, the shapes of both magnetization and resistance curves are similar to those found in the present study. The results for specimens previously quenched from the disordered state (600 C) are shown by curves A and A' of Fig. 11 and do not agree well with those found in the present study. On the other hand, both magnetization and resistance curves for specimens previously partially ordered (curves B and B' of Fig. 11) show a satisfactory agreement with those found in this study under similar condition.

B. AuCu

As mentioned in section III that the mechanism of isothermal ordering of AuCu may be different in the two temperature ranges, one being near the transition temperature and the other being away from the transition temperature, it is therefore desirable to treat the kinetic data of AuCu separately in these two temperature regions.

i. Near the transition temperature (350 to 408 C)

a. Heat of evolution

The internal energy of an alloy is decreased during the ordering process as disordered regions change to ordered regions. If the released energy is measured at constant temperature, it can be used as measure of the fraction of ordered mass present in the specimen.

Nyström's data (6) for the heat of evolution, U/U_{∞} versus log time, are shown in Fig. 12. In order to analyze these data as was done for $MnNi_3$ in the previous section, the data of heat of evolution are now plotted as $\ln\ln 1/(1-U/U_{\infty})$ vs. $\ln(t)$ in Fig. 13. Two straight lines can be fitted to these data with slopes 4 (dashed line) and 2.5 (full line) for the beginning and the second part of the ordering process respectively. The straight line of slope 4 corresponds to the period during which constant nucleation and constant radial growth of ordered spherical nuclei are operative (23). This interpretation of constant nucleation and constant growth was also mentioned by

Nystrom in his original paper (6). In the second part of the ordering process, the straight lines having slope 2.5 correspond to the growth of the plate-like ordered domains, since generally the growth of the plate-like transformed mass in the untransformed matrix is proportional to the 2.5 power of the time of the reaction (22). The plate-like shape of ordered domains may be necessary in order to give the least strain energy during the growth of the tetragonal ordered structure in the matrix of cubic disordered structure. This possibility was qualitatively discussed and experimentally verified by a study of microstructure and x-ray diffraction patterns in Marker's paper (11) for AuCu and by Newkirk et al in their paper (12) on CoPt.

b. Intensities of x-ray diffraction lines.

The intensities of reflections from ordered and disordered planes having the same Miller indices should be proportional to the mass of the ordered and disordered regions respectively.

Borelius' results (8) of intensity, $I_o/(I_o+I_d)$ versus log time, are shown in Fig. 14. As was done in the case of the heat of evolution, these data are plotted as $\ln\ln(1-i)^{-1}$ vs. $\ln(t)$ in Fig. 15. The parameter i used in Fig. 15 is equal to $(1.5I_o)/(1.5I_o+I_d)$ instead of $I_o/(I_o+I_d)$, since the original (311) cubic reflection separates into the tetragonal reflections (311) and (113),

and the multiplicity factors of these two latter reflections are in the ratio of 2 to 1.

The significant result of this analysis is that the slope of the straight lines in Fig. 15 is 2.5 and this result agrees quite well with that based on heat of evolution measurements.

ii. Low temperature range (150 to 350 C) from measurement of the displacement of (311) diffraction line.

The shift of the ordered tetragonal (311) line during the ordering process may mean that local ordering occurs homogeneously all over the specimen in this range of ordering temperatures.

In Fig. 16 are shown data from Borelius' measurements (8) of the distance D between the ordered (311) reflection and the (222) reflection, which remains essentially fixed and thus was used as a reference line. In order to analyze the data as was done for $MnNi_3$ in the previous section, the data of displacement of (311) line are now plotted as ln(1-s) vs. ln(t) in Fig. 17. The parameter s is equal to $(D-D_i)/(D_e-D_i)$ and is the fraction of change of position of (311) line. Thus s has the value zero at the beginning of the process, where $D=D_i$; and has the value one at the end of the process, where $D=D_e$. As shown in Fig. 17 the data can be fitted by straight lines with slope equal to -0.75. The differential form of this

straight line is:

$$\Delta s = \text{const.}\ \Delta(t^{-0.75}) \qquad (12)$$

Equation (12) may now be explained. From the geometry of the x-ray camera, the change in position of the (311) reflection line is proportional to the change in Bragg angle θ_{311}. Hence Δs is proportional to ΔD, which is proportional to $\Delta\theta_{311}$. For small change of Bragg angle, $\Delta\theta_{311}$ is proportional to $\Delta(\sin\theta_{311})$, and according to Bragg's Law, $\sin\theta_{311}$ is proportional to $1/d_{(311)}$. If we assume that the change in the (311) interplanar spacing $d_{(311)}$ is proportional to the change of the ordered fraction, which according to expression (3) in section VI is proportional to the square root of the number of atoms n in the fluctuating group, then

$$\Delta\left[1/d_{(311)}\right] \sim \Delta\left(1/n^{\frac{1}{2}}\right) \sim \Delta(n)^{-\frac{1}{2}} \sim \Delta\left[(t^{1.5})^{-\frac{1}{2}}\right] \sim \Delta\,(t^{-0.75})$$

is proportional to the right side of equation (12). This analysis provides a physical interpretation for equation (12), and confirms the homogeneous ordering of AuCu in this temperature range.

C. CoPt

Only resistance measurements were analyzed from the study of CoPt by Newkirk et al (12), because the hardness and magnetic measurements have large scattering.

Resistance data for CoPt (48 atomic per cent Co) are shown in Fig. 18. As was done for the data on the resistance of $MnNi_3$ in section VI, the resistance data of CoPt are plotted in Fig. 19. Fig. 19, as Fig. 10, shows the linearity of experimental data when plotted as

$$\ln\ln 1/(1-\frac{R - R_i}{R_1 - R_i}) \text{ vs. } \ln(t) \text{ and } \ln(1-\frac{R - R_i}{R_2 - R_i}) \text{ vs. } \ln(t)$$

for the first and the second step of the ordering process respectively. The resistance data in these two parts of the plot are also fitted by straight lines with slope 1.25 and -0.5 respectively. Since the physical property measured, the coordinates of the plot and the slope of the straight lines are same in both Fig. 19 for CoPt and Fig. 10 for $MnNi_3$, the description of ordering mechanism used for the alloy $MnNi_3$ may be also applied to the alloy CoPt.

D. $AuCu_3$

No attempt has been made to analyze the curve of resistance versus time in Sykes's paper published in 1936 (16), since the time scale used there was linear and only one curve was available.

In a later paper (15) Sykes studied the size of ordered nuclei in $AuCu_3$ as a function of time. His measurements are replotted in Fig. 20. From this plot it can be seen that the data may be fitted by a straight line with a slope equal to 0.5. Because of the similitude in structure between $AuCu_3$ and $MnNi_3$, this time dependence of the size of the ordered domain of $AuCu_3$ may be extended to $MnNi_3$. Fig. 20 thus constitutes experimental evidence of the assumption used in section VI for the purpose of explaining the ordering kinetics of $MnNi_3$.

As Sykes mentioned in his paper (15), the change of resistance of $AuCu_3$ is inversely proportional to the change of the size of ordered nuclei for the later part of the ordering process. If this result is combined with the time dependence of the size of the ordered nuclei as given by Fig. 20, it can be seen that the change of resistivity of ordered $AuCu_3$ is proportional to the change of $t^{-\frac{1}{2}}$ during the later part of the ordering process as in the cases of $MnNi_3$ and CoPt.

VIII. Conclusions

This work establishes procedures of analysis and interpretation of isothermal ordering data for $MnNi_3$, AuCu, CoPt and $AuCu_3$ and thus provides a technique by which the mechanism of ordering may be understood.

These analyses indicate that at least three mechanisms may be operative during the ordering process, as summarized below.

A. Nucleation and Growth (as ordering of AuCu near the transition temperature).

The ordering process starts with a constant nucleation rate, the rate of forming nuclei per unit disordered volume being constant. At the same time, the ordered nuclei grow radially at a constant rate. After nucleation ceases, the ordered nuclei continue to grow in the disordered matrix according to some definite time relationship; an example of this process is given by the plate-like growth of AuCu near the transition temperature.

B. Random Local Ordering and then Growth of Anti-phase Ordered Domains (as $MnNi_3$ and possibly $AuCu_3$ and CoPt)

Local ordering, which is described by the sharpening of Gaussian distribution curve of local composition in this work, occurs randomly in the disordered matrix until the entire specimen is filled with anti-phase

ordered domains, which have the equilibrium state of order for the ordering temperature. Then, by the growth of some domains, the disordered domain boundaries are gradually eliminated.

C. Uniform Ordering (as AuCu at low temperature)

The whole specimen is being uniformly ordered during the ordering process. This is the case of AuCu at temperatures relatively low with respect to the transition temperature.

Nomenclature

a	Lattice parameter
c	Lattice parameter
D	Distance between (311) and (222) x-ray diffraction lines on the film, with subscripts i and e referring to values near the beginning and the end of the isothermal ordering process
d	Number of atoms along an edge of the cubic ordered domain
$d_{(311)}$	Interplanar spacing of (311) planes
e	Thickness of disordered domain-boundary of the ordered domains
f	Free energy per atom
f_1	Dimensionless parameter representing the fractional change in magnetization readings during the first stage of the isothermal ordering process of $MnNi_3$.
f_2	Dimensionless parameter representing the fractional change in magnetization readings during the entire isothermal ordering process of $MnNi_3$
I	Intensity of x-ray diffraction line, with subscripts o and d to represent that of the ordered and disordered reflections respectively
i	Dimensionless parameter, equal to $(1.5I_o)/(1.5I_o+I_d)$, representing the fractional change in intensity of the ordered reflection during the ordering process.

k Boltzmann constant

M Magnetization reading; with subscripts i, 1 and 2 referring to values near the beginning, the end of the first stage of, and the end of the entire ordering process respectively.

n Number of atoms involving in the fluctuating group

N_e Nucleation rate, number of ordered nuclei formed per unit ordering time.

P Probability of a fluctuating group having composition between $(w+\Delta w)$ and $(w+\Delta w)+dw$

R Resistance of ordered specimen; with subscripts m,i, 1 and 2 referring to values near the maximum, the beginning of, the end of the first stage of, and the entire ordering process respectively.

r_1 Dimensionless parameter representing the fractional change in resistance during the first stage of the isothermal ordering process.

r_2 Dimensionless parameter representing the fractional change in resistance during the entire isothermal ordering process.

s Dimensionless parameter representing the fractional shifting of (311) x-ray diffraction line.

T Temperature of the alloy in degree Kelvin

t Time at the ordering temperature.

U Heat of evolution of the ordered alloy, with subscript ∞ referring to the heat of evolution during the entire isothermal ordering process

V Difference of binding energies, $\frac{1}{2}(V_{AA}+V_{BB})-V_{AB}>0$, where V_{AA}, V_{BB} and V_{AB} are binding energies between pairs of A-A, B-B and A-B atoms respectively

z Coordination number, the number of nearest neighbouring atoms

$\theta_{(311)}$ Bragg angle of reflection from (311) planes

References

1. Tammann C., "Zum Gedächtnis der Entdeckung des Isomorphismus vor 100 Jahren, Die chemischen und galvanischen Eigenschaften von Mischkristallreihen und ihre Atomverteilung", Zeits. f. anorg. allgem. Chemie 107, 1 (1919)

2. Bain E. C., "Cored Crystals and Metallic Compounds" Chem. & Met. Eng. 28, 65 (1923)

3. Johansson C. H. and Linde J. O., "Röntgenographische Bestimmung der Atomanordnung in den Mischkristallreihen Au-Cu und Pd-Cu", Ann. d. Physik 78, 439

4. Nix F. C. and Shockley W., "Order-Disorder Transformation in Alloys", Rev. Mod. Phy. 10, 1 (1938)

5. Lipson H., "Order-Disorder Changes in Alloys", Progress in Metal Physics Vol. 2 (1950)

6. Nyström J., "A Calorimetric and Resistometric study on the transformations in AuCu", Arkiv för Fysik, 2, 151 (1950)

7. Borelius G., Larsson L. E. and Selberg H., "Evolution of Heat during Disorder-Order Transformations in AuCu", Arkiv för Fysik 2, 161 (1950)

8. Källbäck O., Nyström J. and Borelius G., "Kinetics of the Order-Disorder Transformations in CuAu", Ing. Vetensk. Akad., Handl., 157, 21 (1941)

9. Diennes G. J., "Kinetics of Ordering in the Alloy AuCu", Jour. App. Phy., 22, 1020 (1951)

10. Gorsky W. S., "On the Transitions in the AuCu Alloy", Physik. Z. Sowjetunion, 6, 69 (1934)

11. Harker D., "Order Hardening: Its Mechanism and Recognition", Trans. Amer. Soc. Metals 32, 210 (1944)

12. Newkirk J. B., Geisler A. H., Martin D. L. and Smoluchowski R., "Ordering Reaction in Cobalt-Platinum Alloys", Jour. of Metals 188, 1249 (1950)

13. Nowack L., "Vergütbare Edelmetall-Legierungen", Zeit. f. Metallkunde 22, 94 (1930)

14. Sykes C. and Jones F. W., "The Atomic Rearrangement Process in the Copper-Gold Alloy Cu_3Au", Proc. Roy. Soc. A, 157, 213 (1936)

15. Jones F. W. and Sykes C., "Atomic Rearrangement Process in the Copper-Gold Alloy Cu_3Au II", Proc. Roy. Soc. A, 166, 376 (1938)

16. Sykes C. and Evans H., "The Transformation in the Copper-Gold Alloy Cu_3Au", J. Inst. Met. 58, 255 (1936)

17. Siegel S., "On the Kinetics of the Order-Disorder Transformation in Cu_3Au", J. Chem. Phys. 8, 860 (1940)

18. Thompson N., "The Order-Disorder Transformation in the Alloy Ni_3Mn", Proc. Phys. Soc., London, 52, 217 (1940)

19. Köster W. and Rauscher W., "Beitrag zum System Nickel-Mangan", Z. Metallkunde 39, 178 (1948)

20. Cotrell A. H., Theoretical Structural Metallurgy. 230 to 232. Edward Arnold & Co. (1948)

21. Smouchowski R., "Influcence of Order on Magnetic Properties", Le Journal de Physique et le Radium Vol. 12, No. 3, 389 (1951)

22. Zener C., "Theory of Growth of Spherical Precipitates from Solid Solution", Journal of App. Phys., 20, 950 (1949)

23. Johnson W. A. and Mehl R. F., "Reaction Kinetics in Process of Nucleation and Growth", American Institute of Mining and Metallurgical Engineers Transition, (iron and steel division) vol. 135, 416 (1939)

Fig. 1 Ordered Crystal Structures

AB - Type

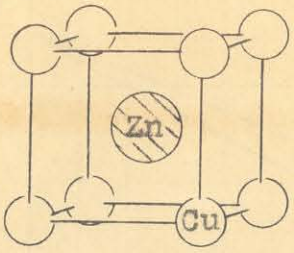

i. Ordered CuZn

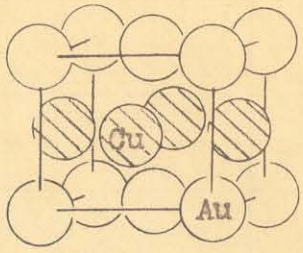

ii. Ordered AuCu or CoPt

AB_3 - Type

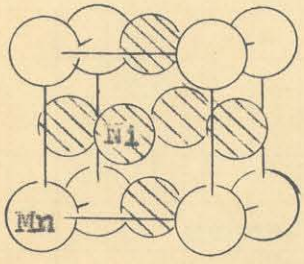

i. Ordered $AuCu_3$ or $MnNi_3$

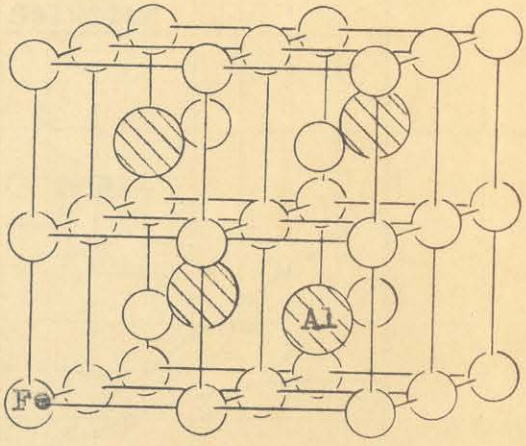

ii. Ordered Fe_3Al

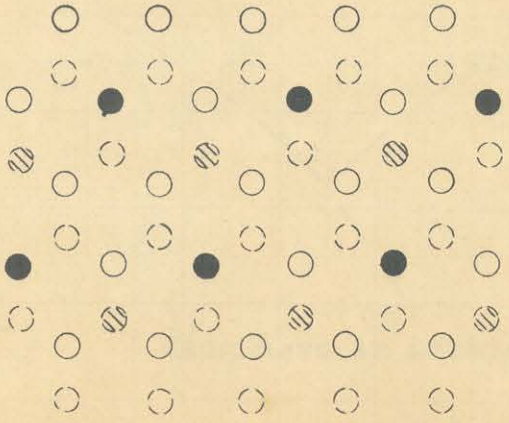

Mg	Cd	
○	●	Atoms in even planes
○	⊘	Atoms in odd planes

iii. Ordered Mg_3Cd

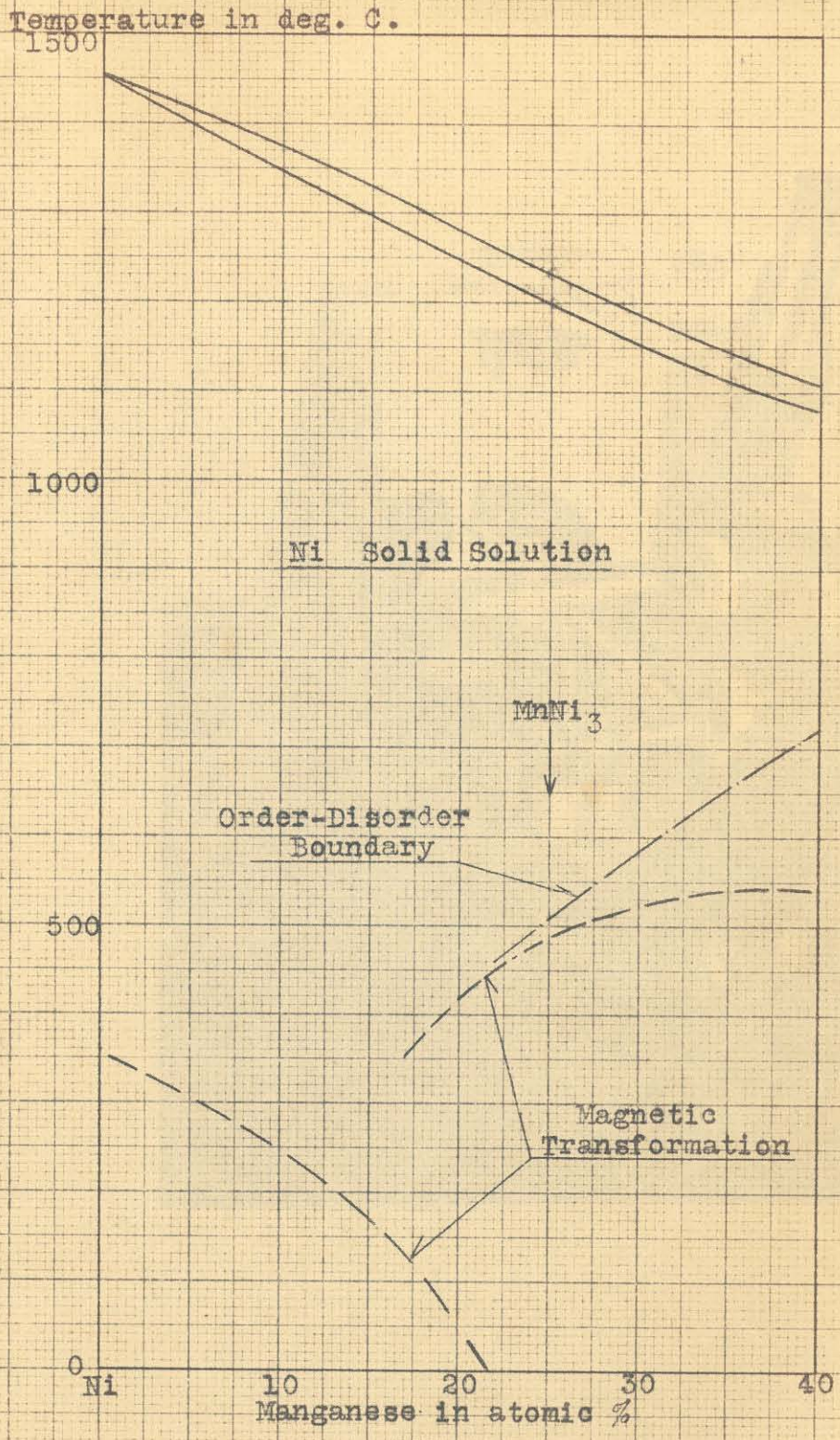

Partial Manganese Nickel Phase Diagram

Fig. 2

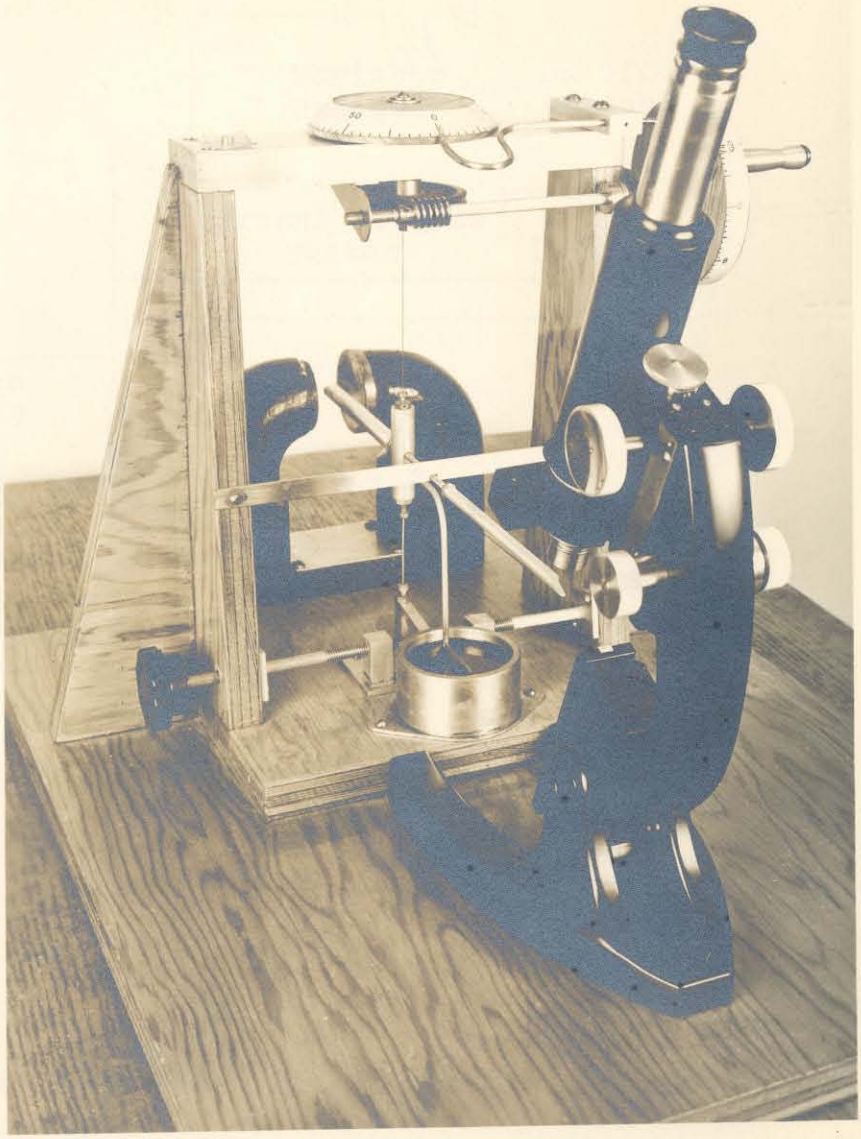

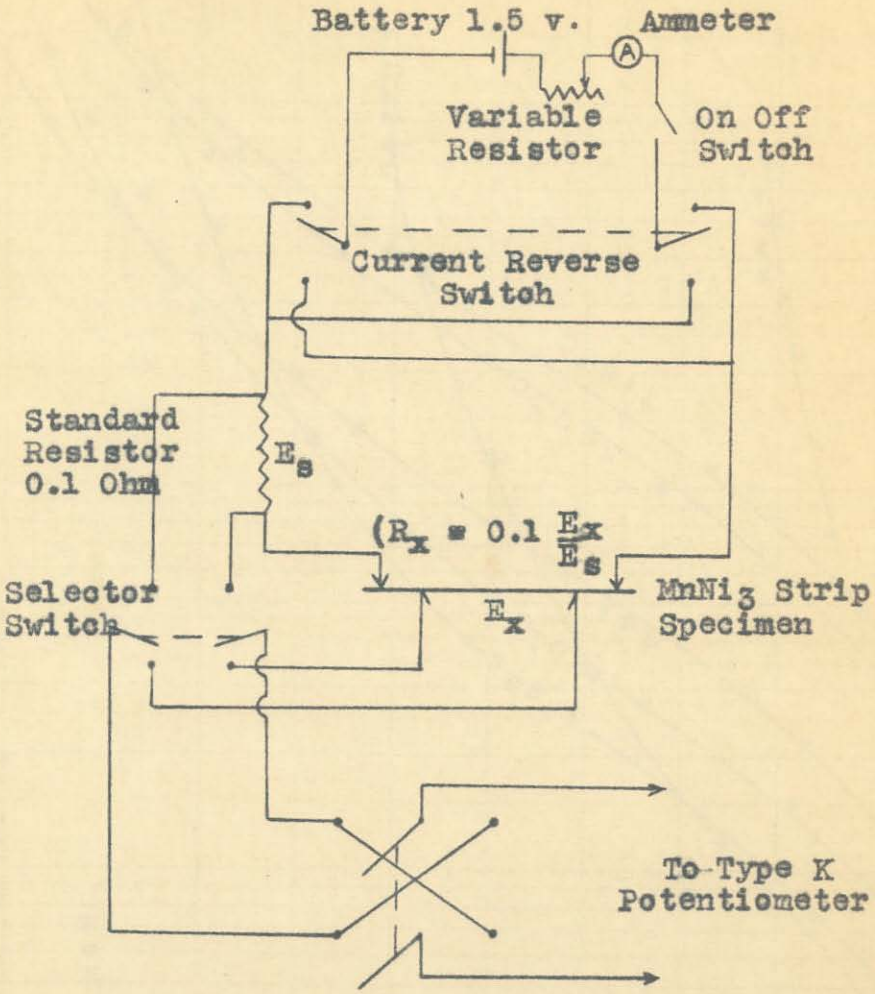

Wiring Diagram For Resistance Measurement

Fig. 4

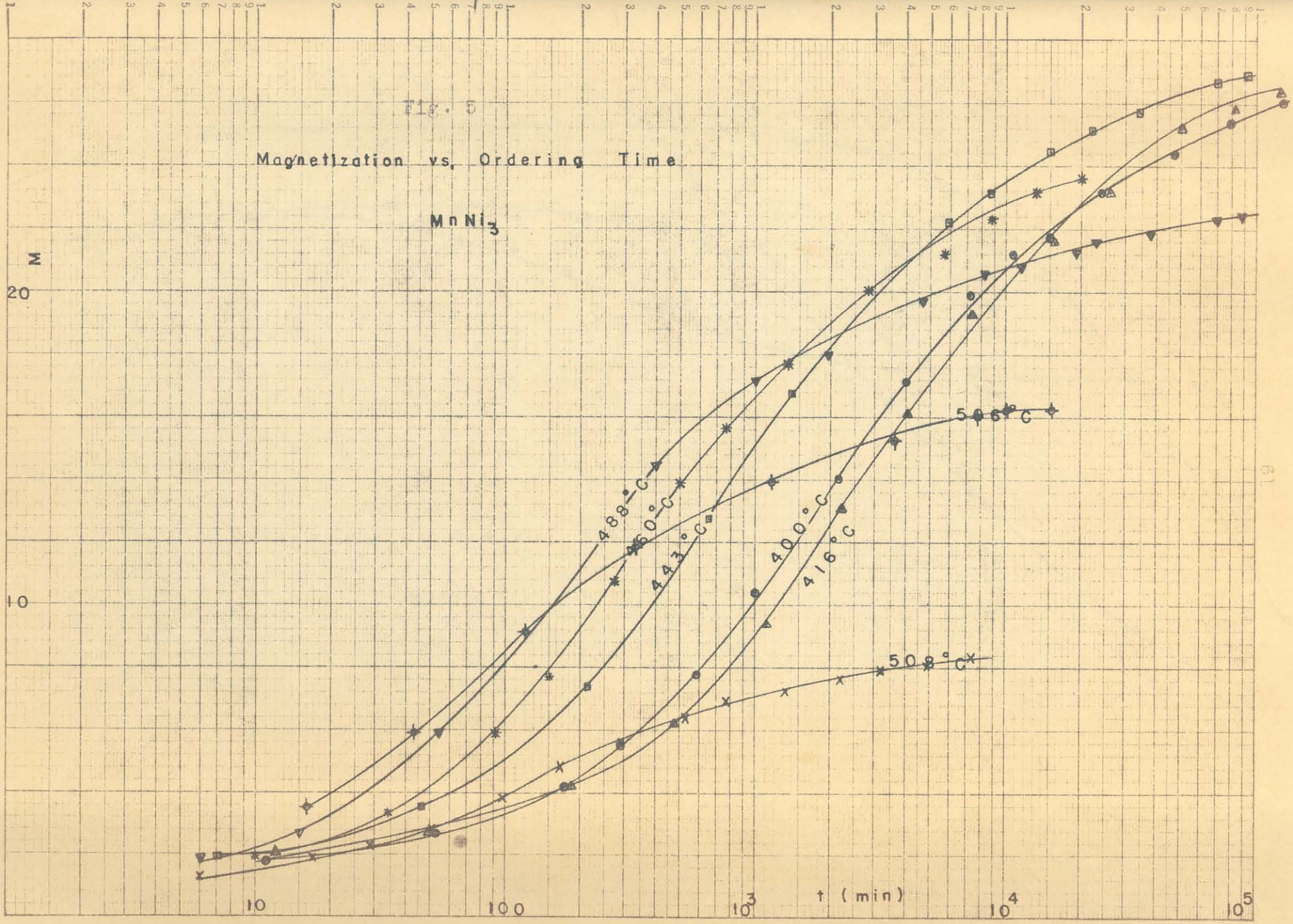
Magnetization vs. Ordering Time
$MnNi_3$
M
20
10
488°C
460°C
443°C
400°C
416°C
506°C
508°C
10
100
10^3
t (min)
10^4
10^5

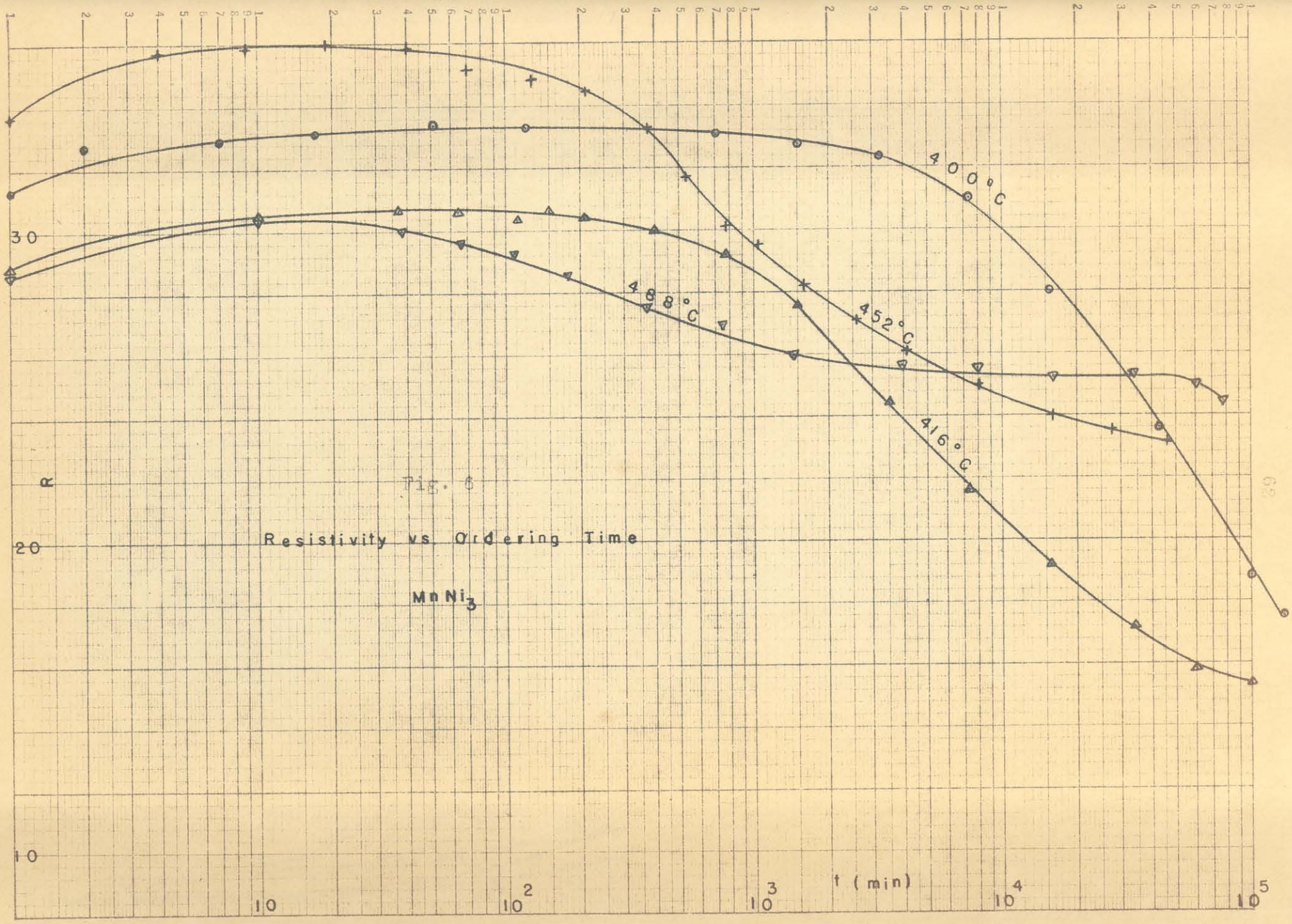

Fig. 6

Resistivity vs. Ordering Time

$MnNi_3$

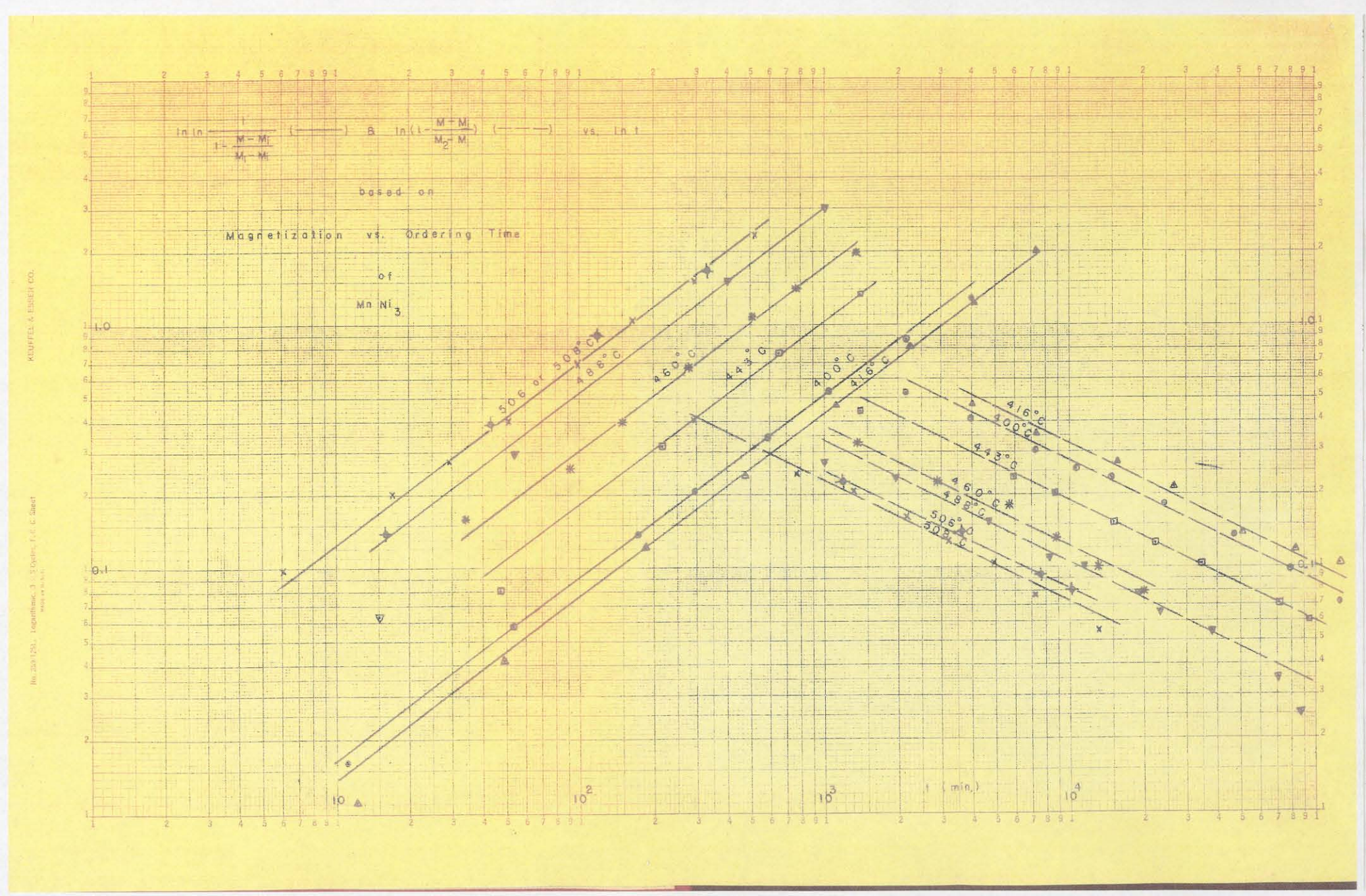
$\ln \ln \frac{1}{1-\frac{M-M_i}{M_f-M_i}}$ (———) & $\ln\left(1-\frac{M+M_i}{M_2-M_i}\right)$ (— — —) vs. ln t
based on
Magnetization vs. Ordering Time
of
Mn Ni3
506 or 508°C
498°C
460°C
443°C
400°C
416°C
416°C
400°C
443°C
460°C
498°C
506°C
508°C
1.0
0.1
10
10^2
10^3
10^4
t (min.)

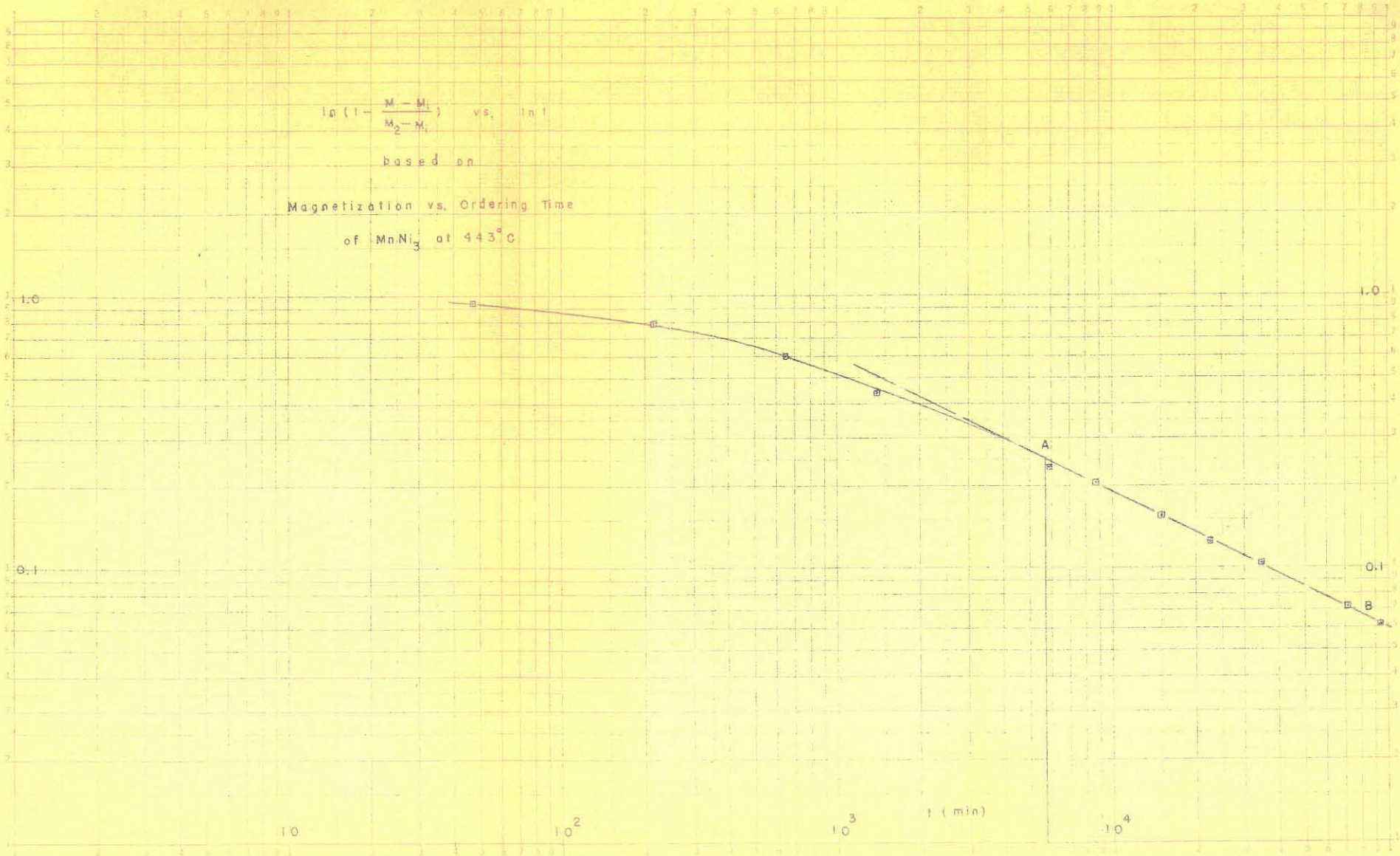
$\ln\left(1-\frac{M-M_i}{M_2-M_i}\right)$ vs. $\ln t$
based on
Magnetization vs. Ordering Time
of $MnNi_3$ at 443°C
1.0
0.1
A
B
10
10^2
10^3
10^4
t (min)

Fig. 9

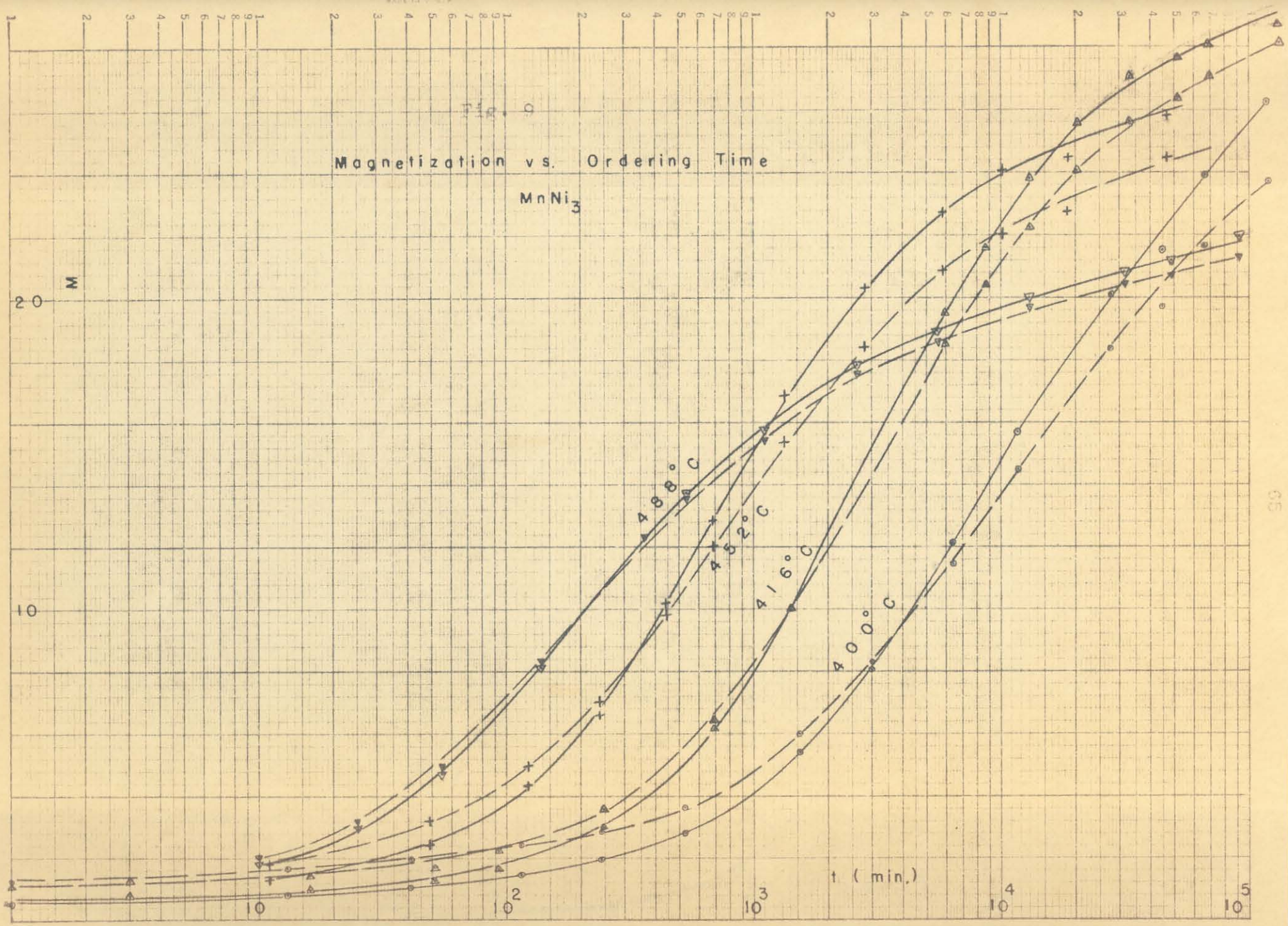
Magnetization vs. Ordering Time
MnNi3
M
20
10
488° C
452° C
416° C
400° C
t (min.)
10
10^2
10^3
10^4
10^5

$\ln \ln \frac{1}{1 - \frac{R - R_m}{R_1 - R_m}}$ (———) & $\ln \left(1 - \frac{R - R_m}{R_2 - R_m}\right)$ (— — —) vs. $\ln t$

based on

Resistivity vs. Ordering Time

of

$MnNi_3$

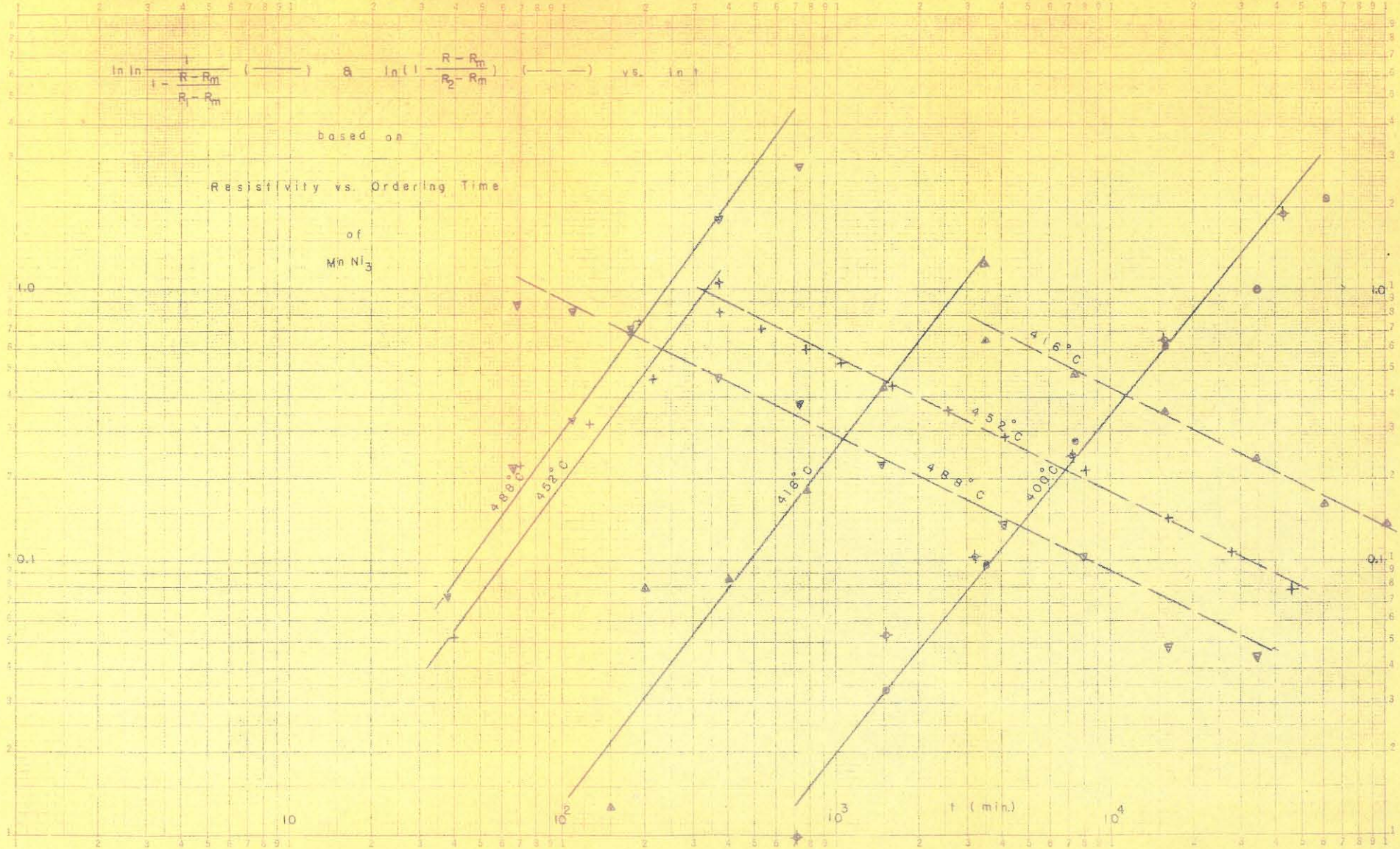

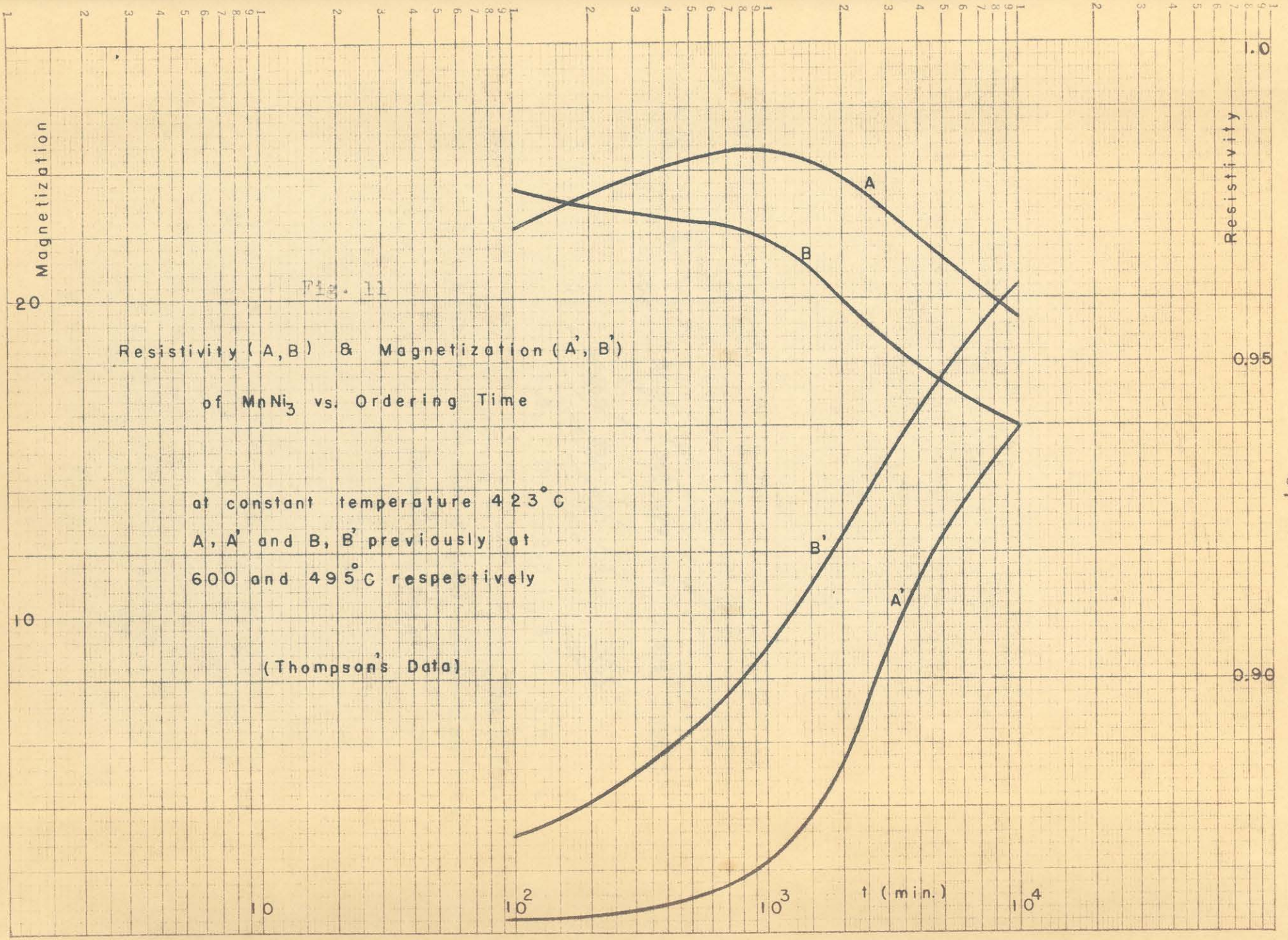

Fig. 11

Resistivity (A, B) & Magnetization (A', B')

of $MnNi_3$ vs. Ordering Time

at constant temperature 423°C

A, A' and B, B' previously at

600 and 495°C respectively

(Thompson's Data)

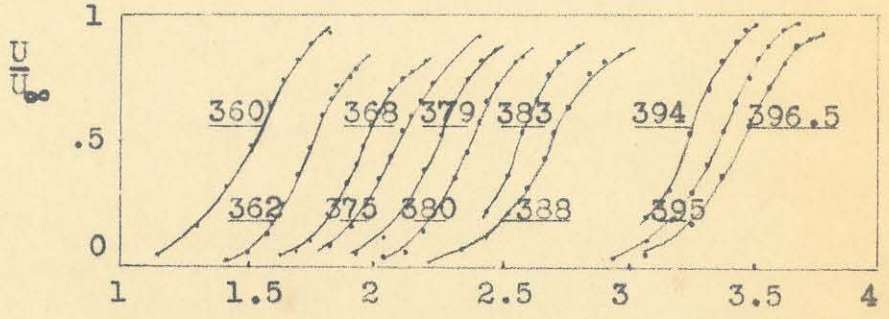

Heat of evolution of AuCu vs. heating time

(Nyström's Data)

Fig. 12

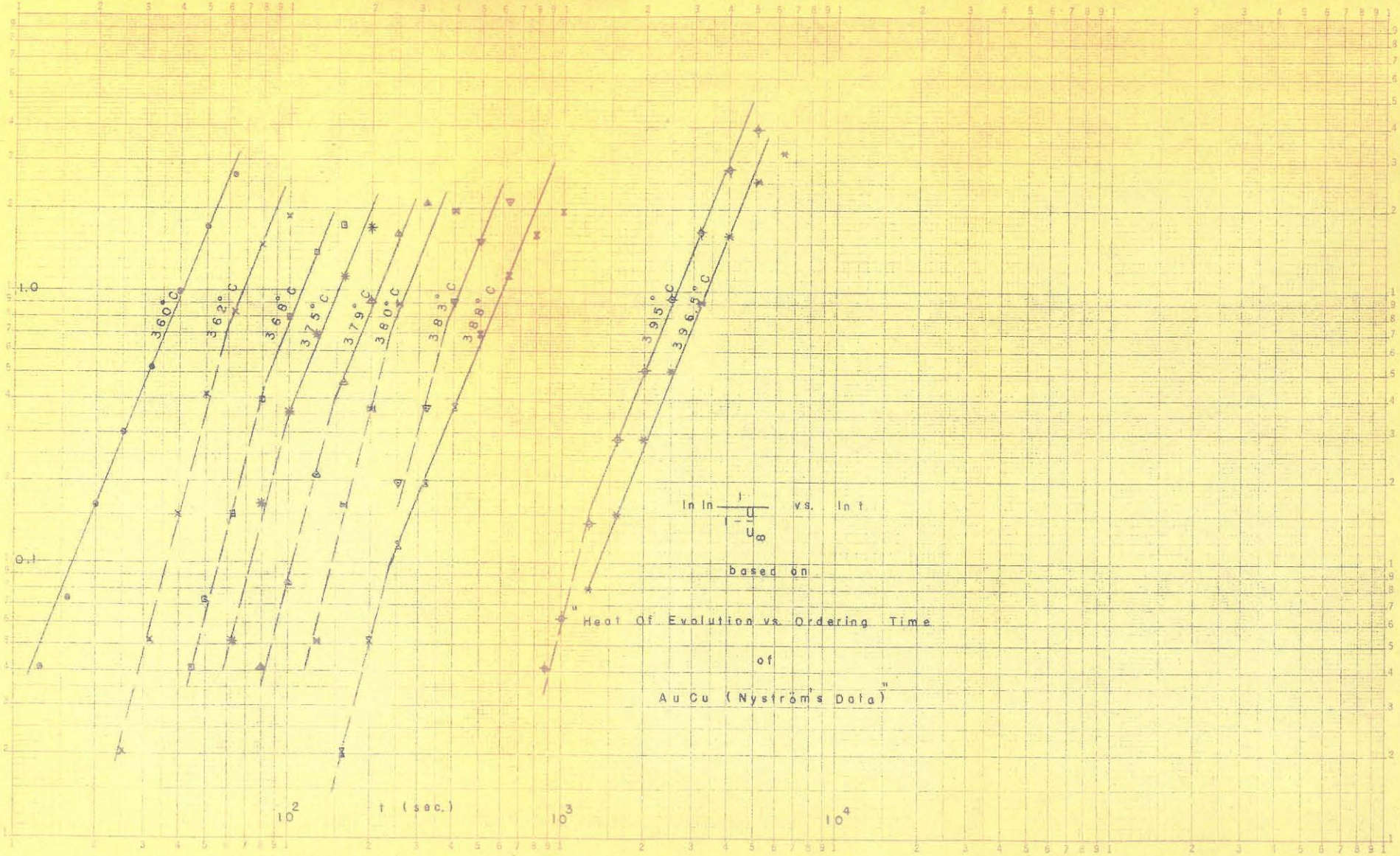
360°C
362°C
368°C
375°C
379°C
380°C
383°C
388°C
395°C
396.5°C
1.0
0.1
10^2
10^3
10^4
t (sec.)
$\ln \ln \frac{1}{1-U}$ vs. ln t
U_∞
based on
"Heat Of Evolution vs. Ordering Time
of
Au Cu (Nyström's Data)"

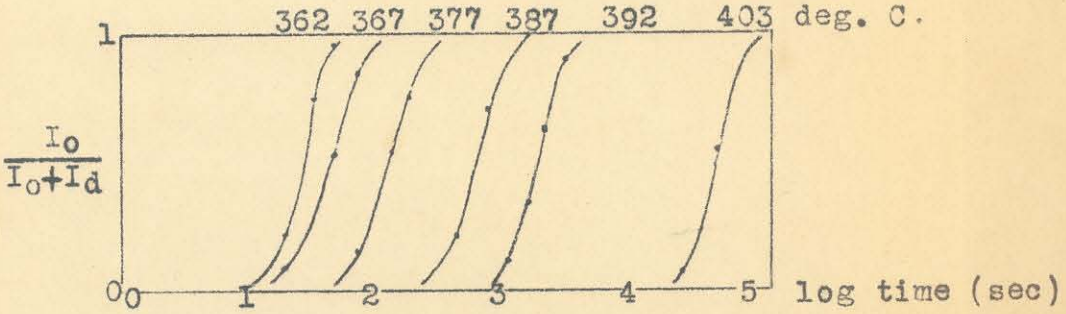

Intensity of the line (311) of AuCu versus logarithms of heating times (Borelius' Data)

Fig. 14

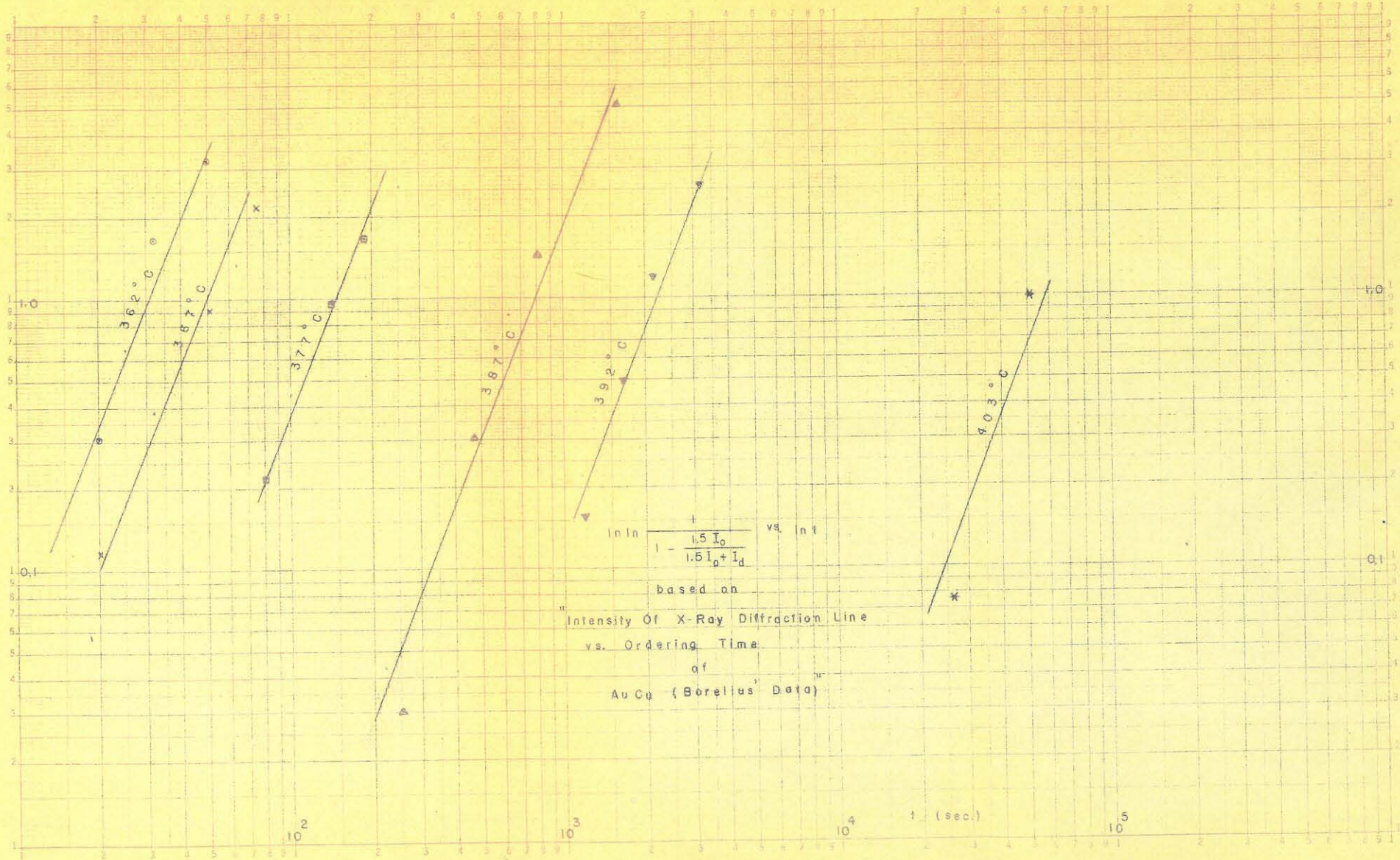
1.0
0.1
362° C
387° C
377° C
397° C
392° C
403° C
$\ln \ln \frac{1}{1 - \frac{1.5\,I_o}{1.5\,I_o + I_d}}$ vs. $\ln t$
based on
Intensity Of X-Ray Diffraction Line
vs. Ordering Time
of
Au Cu (Borelius' Data)
10^2
10^3
10^4
10^5
t (sec.)

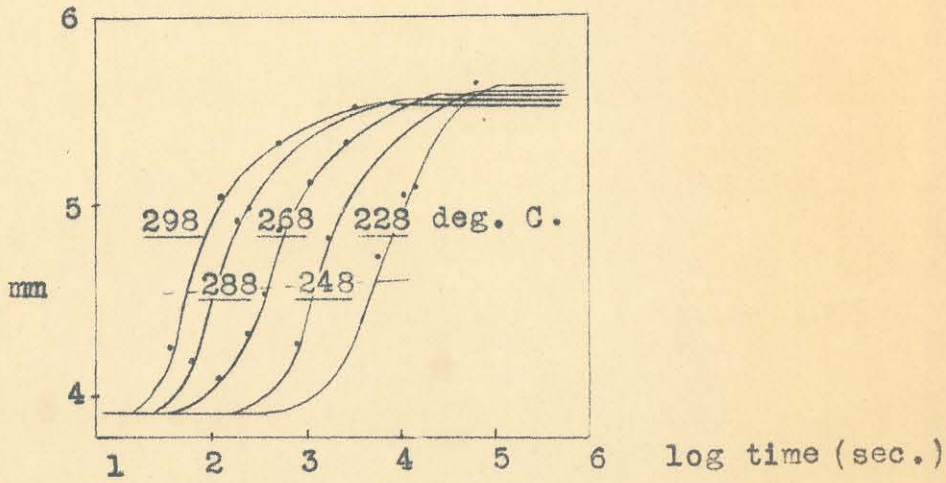

Distance of the lines (311) and
(222) vs. logarithms of heating times
(Borelius' Data)

Fig. 16

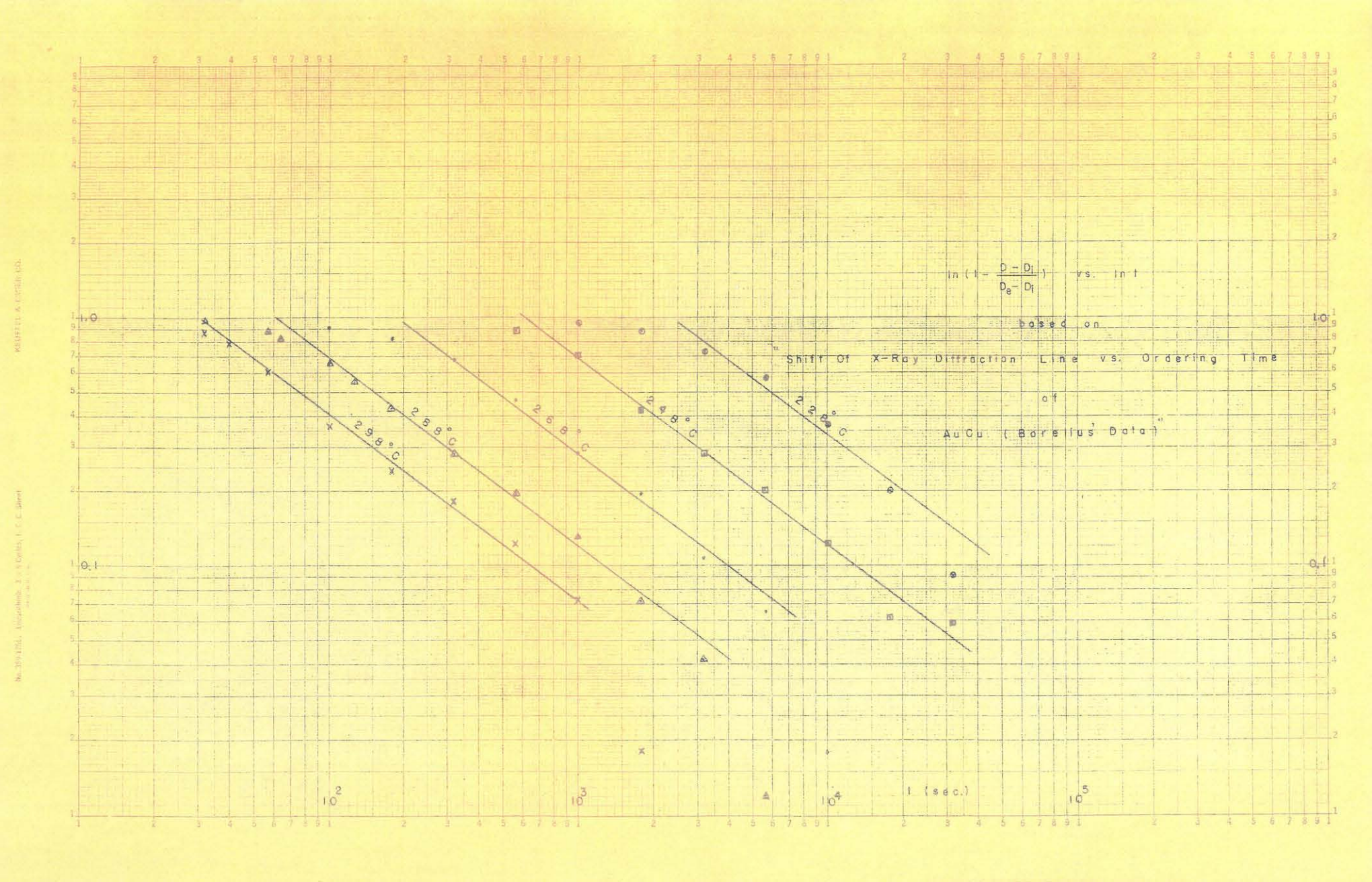
$\ln\left(1-\frac{D-D_i}{D_e-D_i}\right)$ vs. $\ln t$
based on
"Shift Of X-Ray Diffraction Line vs. Ordering Time
of
AuCu (Borelius' Data)"
228° C
258° C
288° C
1.0
0.1
10^2
10^3
10^4
10^5
t (sec.)

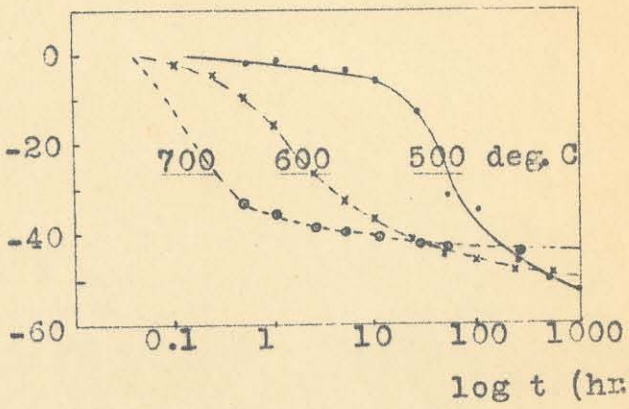

Per cent change in 0 deg. C resistance of 48 atomic % Co alloy vs. time (Newkirk's Data)

Fig. 18

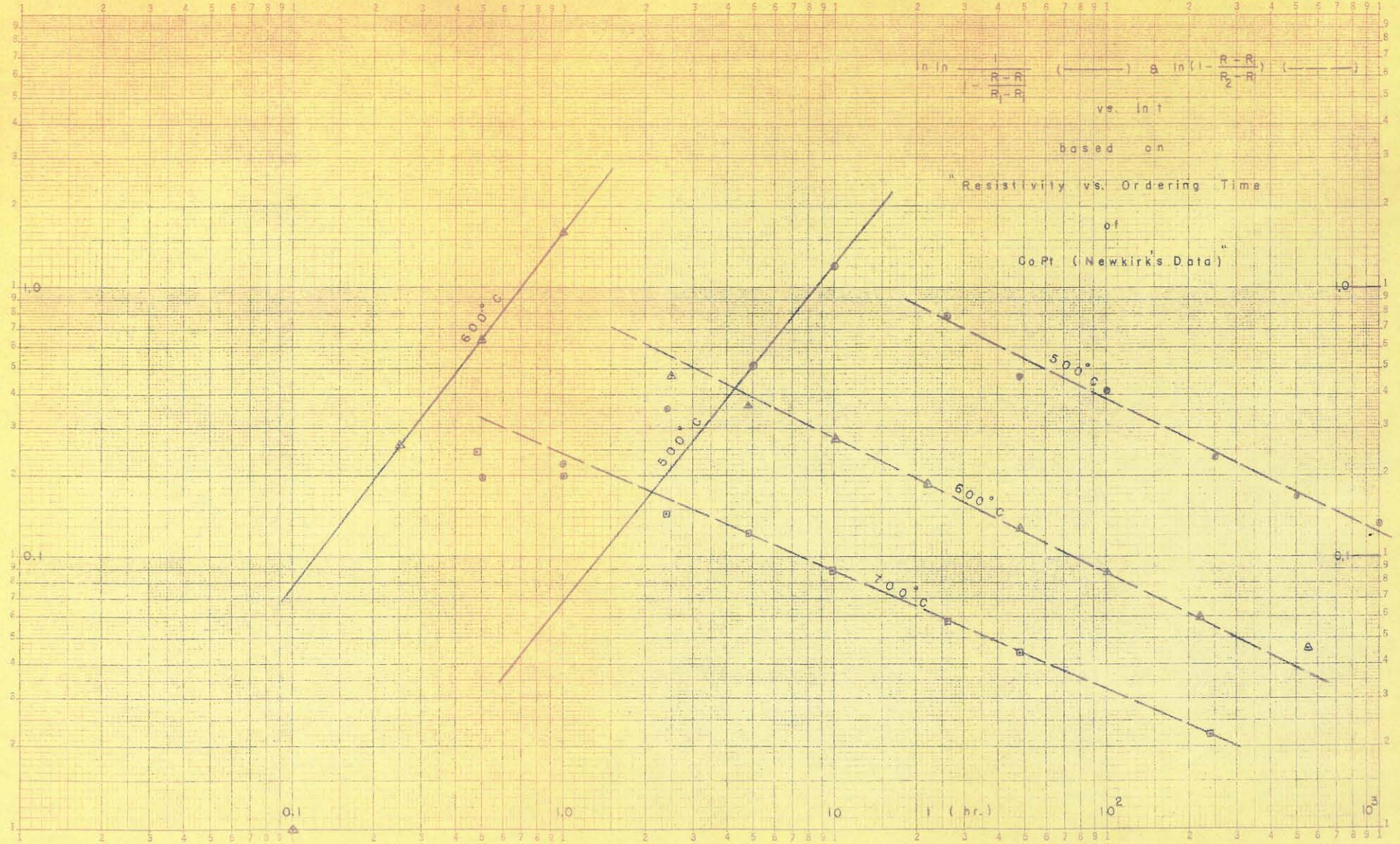
$\ln \ln \frac{1}{1-\frac{R-R_1}{R_2-R_1}}$ ( ) & $\ln(1-\frac{R-R_1}{R_2-R_1})$ ( )
vs. ln t
based on
"Resistivity vs. Ordering Time of CoPt (Newkirk's Data)"
600° C
500° C
500° C
600° C
700° C
1.0
0.1
0.1
1.0
10
1 (hr.)
10^2
10^3

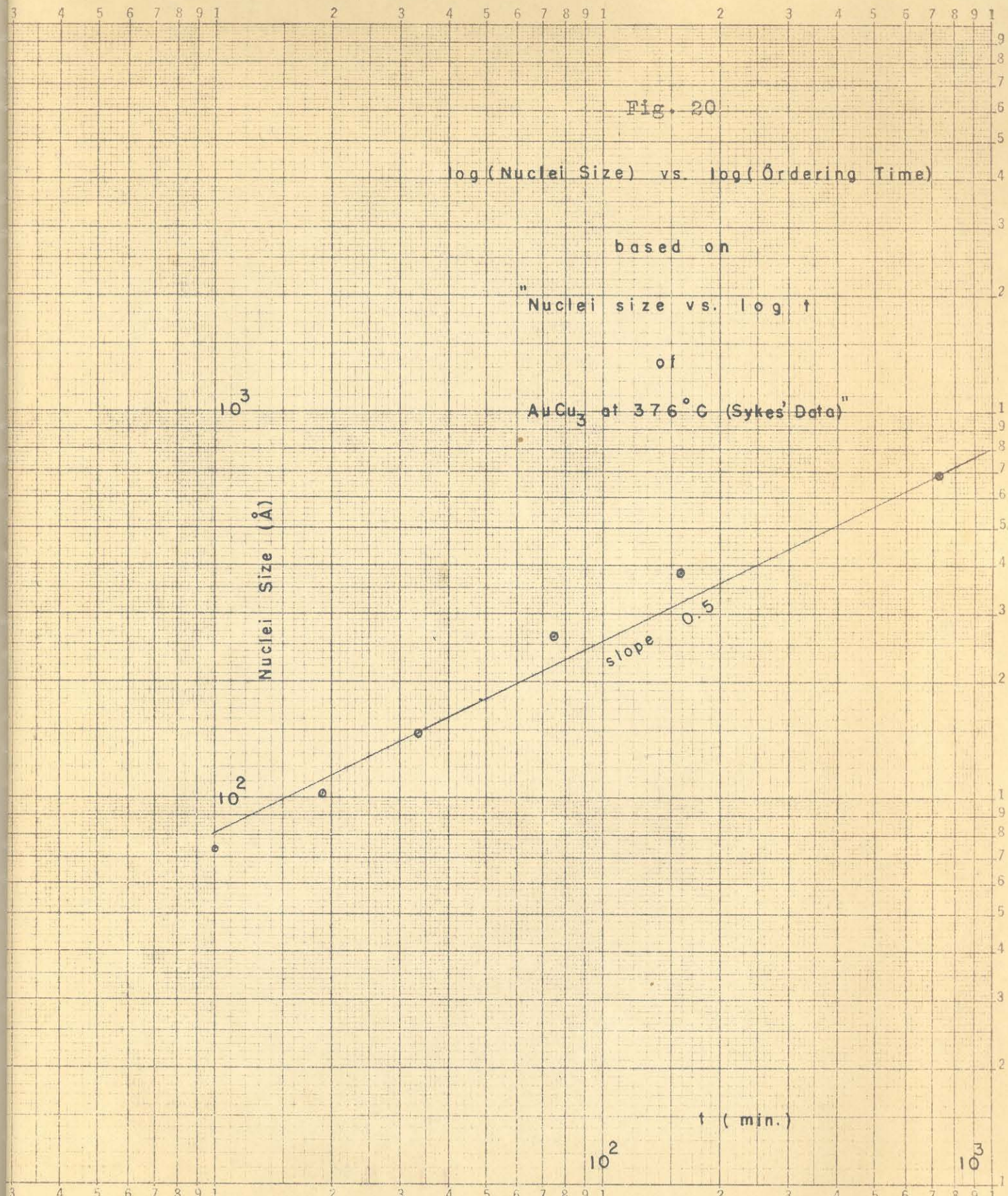
Fig. 20
log (Nuclei Size) vs. log (Ordering Time)
based on
"Nuclei size vs. log t
of
AuCu3 at 376°C (Sykes' Data)"
Nuclei Size (Å)
10^3
10^2
slope 0.5
t (min.)
10^2
10^3